

Thin Flat Plate With Linear Spring As Mechanical Stop

Federal Manufacturing & Technologies

B. H. Johnson

KCP-613-5035

Published June 1997

Final Report

Approved for public release; distribution is unlimited.

RECEIVED
JUN 09 1997
OSTI



MASTER

Prepared Under Contract Number DE-ACO4-76-DP00613 for the
United States Department of Energy

 **AlliedSignal**
AEROSPACE

DISCLAIMER

This report was prepared as an account of work sponsored by an agency of the United States Government. Neither the United States Government nor any agency thereof, nor any of their employees, makes any warranty, express or implied, or assumes any legal liability or responsibility for the accuracy, completeness, or usefulness of any information, apparatus, product, or process disclosed, or represents that its use would not infringe privately owned rights. The views and opinions of authors expressed herein do not necessarily state or reflect those of the United States Government or any agency thereof.

All data prepared, analyzed and presented has been developed in a specific context of work and was prepared for internal evaluation and use pursuant to that work authorized under the referenced contract. Reference herein to any specific commercial product, process or service by trade name, trademark, manufacturer, or otherwise, does not necessarily constitute or imply its endorsement, recommendation, or favoring by the United States Government, any agency thereof or AlliedSignal Inc.

Printed in the United States of America.

This report has been reproduced from the best available copy.

Available to DOE and DOE contractors from the Office of Scientific and Technical Information, P. O. Box 62, Oak Ridge, Tennessee 37831; prices available from (615) 576-8401, FTS 626-8401.

Available to the public from the National Technical Information Service, U. S. Department of Commerce, 5285 Port Royal Rd., Springfield, Virginia 22161.

A prime contractor with the United States
Department of Energy under Contract Number
DE-ACO4-76-DP00613.

AlliedSignal Inc.
Federal Manufacturing & Technologies
P. O. Box 419159
Kansas City, Missouri
64141-6159

KCP-613-5035
Distribution Category UC-706

Approved for public release; distribution is unlimited.

THIN FLAT PLATE WITH LINEAR SPRING AS MECHANICAL STOP

B. H. Johnson

Published June 1997

Final Report
B. H. Johnson, Project Leader

Project Team:
G. L. Harshman
W. J. Spills

DISTRIBUTION OF THIS DOCUMENT IS UNLIMITED

 **AlliedSignal**
AEROSPACE

DISCLAIMER

Portions of this document may be illegible in electronic image products. Images are produced from the best available original document.

Contents

<i>Section</i>	<i>Page</i>
Abstract	7
Summary	7
Discussion	9
Scope and Purpose	9
Prior Work	9
Activity	9
General	9
Analysis of Infinite Plate	10
Analysis of Finite Plate	27
Discussion of Theoretical Results	39
Device Tested	39
Test Results	42
Theoretical Results	49
Discussion of Results	49
Predictions From the Theory	52
Accomplishments	57
Future Work	57
References	59

Appendices

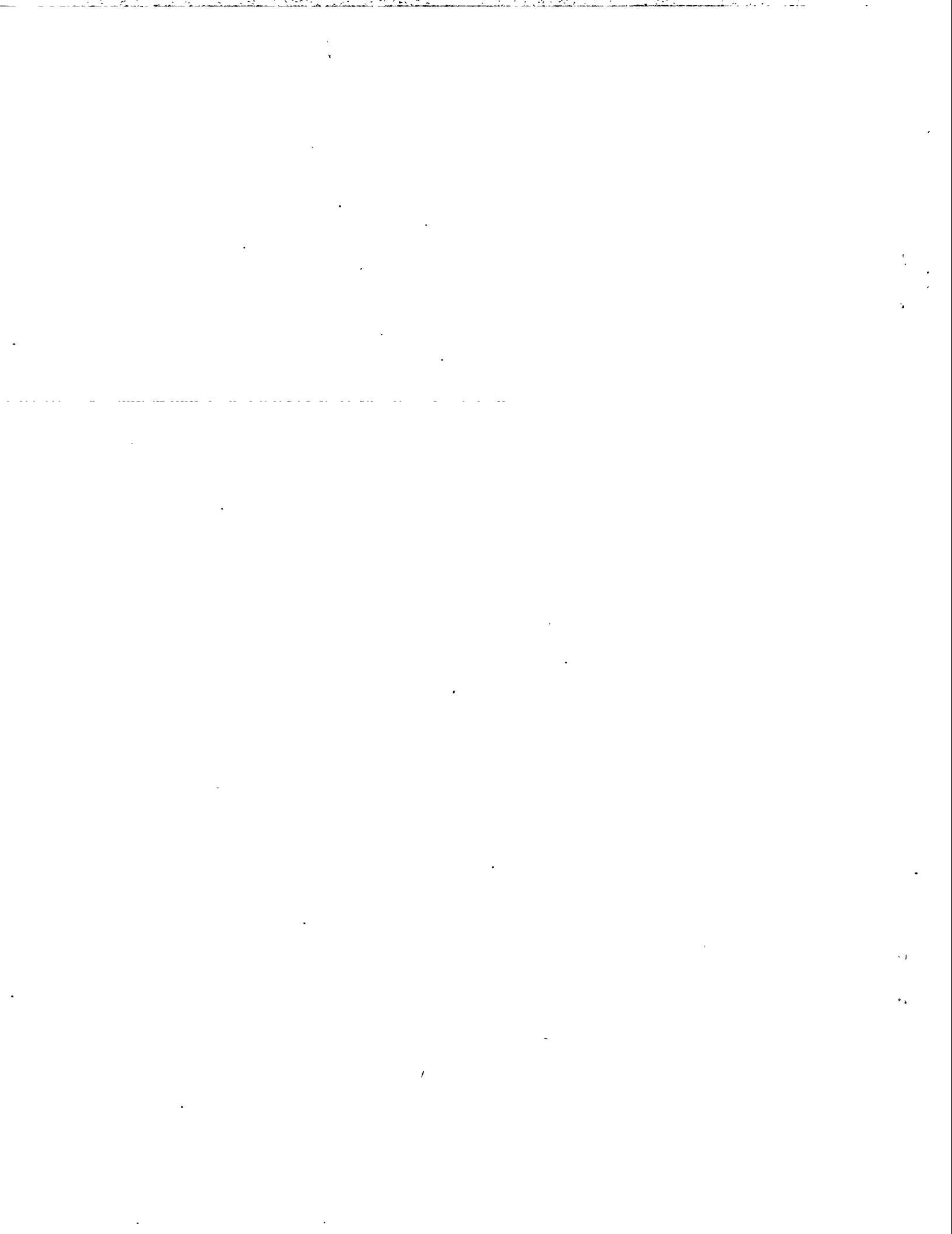
A. Final Report, Thin Flat Plates as Mechanical Stops.....	61
B. Final Report, Dead Mechanism Stop Using Thin Flat Plate	75
C. Equivalence of Impact of Linear and Rotary Object With Flat Plate.....	79
D. Dimensions and Units.....	87
E. Flat Plates Which Cause Cancellation of First Reflections From the Edges.....	95
F. Scaling the Flat Plate Device	101

Illustrations

Figure		Page
1	Elements of the Flat Plate Device During Impact.....	11
2	Free-Body Diagram of Elements During Impact.....	12
3	Determination of Effective Sine Wave of Impact.....	33
4	Pulses in a Taut String.....	35
5	Flat Plate Assembly Tested	40
6	Theoretical and Measured Relative Bounce Heights for Low Spring Rate	50
7	Theoretical and Measured Relative Bounce Heights for Medium Spring Rate.....	51
8	Theoretical and Measured Relative Bounce Heights for High Spring Rate.....	52
C-1	Simplified Sketch With Rotor in Place of Ball	81
C-2	Simplified Sketch With Lever Added	83
E-1	Rectangular Plate With Virtual Support.....	98
E-2	Flat Plate Device for Miniature Mechanism.....	99

Tables

Number		Page
1	Spring Rate Results.....	43
2	Theoretical and Measured Results for Low Spring Rate	44
3	Theoretical and Measured Results for Medium Spring Rate	47
4	Theoretical and Measured Results for High Spring Rate	48



Abstract

A mechanical device has been developed which dissipates mechanical energy simply and reliably, without generating debris. The device basically consists of a stack of thin flat metal layers, forming a flexible plate, and a mechanical spring to buffer the impact of the moving object. Equations have been developed which allow the design of such devices for particular applications.

Summary

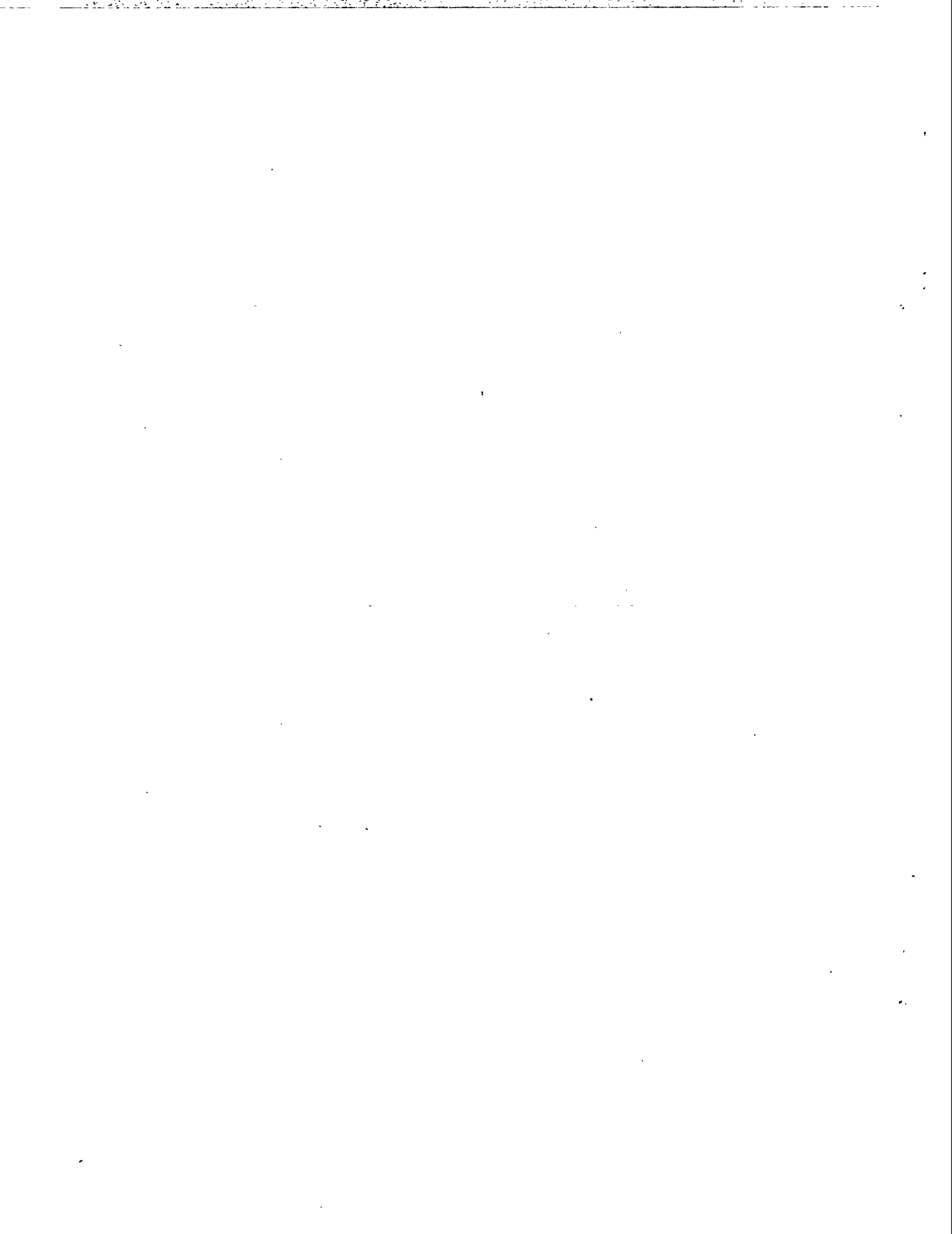
Miniature mechanisms often suffer from excess kinetic energy in moving parts, causing undesirable rebounds, mechanical damage, and debris generation. A simple mechanical device has been developed which can dissipate this kinetic energy without generating debris. The major challenge in utilizing this device is in reducing its volume to an acceptable size. A series of tests coupled with a theoretical analysis has produced a mathematical model which allows an engineer to analytically evaluate various designs to find an optimum configuration.

The tests measured the bounce height of a metal ball dropped onto a laminated plate, impacting an intermediate metal spring. The decay time for the vibration set up in the plate was also measured.

In 1941 Clarence Zener (of Zener diode fame) analyzed the impact of a sphere against an infinitely large thin flat plate and showed that the plate acted as a viscous damper, or dashpot. The local deformation due to contact stresses in the sphere and the plate acted as a nonlinear spring. The resulting differential equation could be numerically evaluated and showed that the sphere separated from the plate when the plate reached its maximum deflection, giving the sphere some predictable rebound velocity. After the rebound, the plate would presumably vibrate and dissipate its energy in internal damping before the sphere would impact it again.

This report considers a small plate with a linear spring. It accounts for the energy which is reflected from the edges of the plate and returns to the impact point and for the velocity of the flexural waves which are set up in the plate. The bounce height as a fraction of the drop height is predicted analytically. The decay time of the plate vibrations is not analyzed.

The theoretical bounce heights agree well with the measured values, indicating that the analysis can be applied to an actual mechanism.



Discussion

Scope and Purpose

The purpose of this project is to tie together the experimental results and a theoretical model of the flat plate device in order to allow an engineer to design such a device for a given application. The kinetic energy which is to be dissipated can be either in the form of linear or rotary motion.

Prior Work

The development of the flat plate device was started as part of the "posigrade cam" redesign effort for a safety "stronglink". That redesign effort was cancelled in 1986, but the development of the flat plate device was continued with a project called "Thin Flat Plates as Mechanical Stops." Additional drop tests of metal balls were conducted and the theory advanced. A copy of the final report of this study is included in Appendix A.

An attempt to use finite element analysis to gain an understanding of the behavior of the flat plate was made in another study, "FEA for Flexural Vibration of Beams." In spite of the title, the analysis progressed to the impact of a mass with the center of a flat plate. The analysis was only partially completed, and it was not obvious how the results could be interpreted usefully.

The development of the flat plate device was continued in the project, "Dead Mechanism Stop Using Thin Flat Plate." As part of this project, a mechanical stop for a module drive arm of another assembly using a flat plate was built and tested. This effort was premature and performed no better than the existing stop. The theory of the device was, however, improved and still appeared to be promising. Another device, involving simpler physics, was built but wasn't tested. In this device, the flat plate served only to dissipate the energy of the impact after the initial rebound. A copy of the final report of this study is included in Appendix B.

Activity

General

In mechanism design, it is generally good practice to have a significant margin between the applied force or torque and the static resisting force or torque in order to ensure

reliable operation. This results in an excess of kinetic energy at the end of the stroke, causing an undesirable rebound, surface wear and even peeling, and debris generation. No device is presently available for cleanly and reliably dissipating this energy in such a way that there is only a small rebound.

In 1986, a redesign effort for a safety device was cancelled, at least partly because we were unable to retard the return of the output switch from its enabled position without quickly destroying the pallet and gear involved. In researching the topic of impacts and coefficients of restitution, we found a reference in a book called *Impact* to an article written by Clarence Zener in 1941 on the ability of thin flat plates to absorb the impact of a sphere with virtually no bounce.^{1, 2} Zener developed a theory for infinitely large plates which seemed to explain the phenomenon and which seemed to present a solution to our problem--if we could find a way to reduce the plate to a reasonable size.

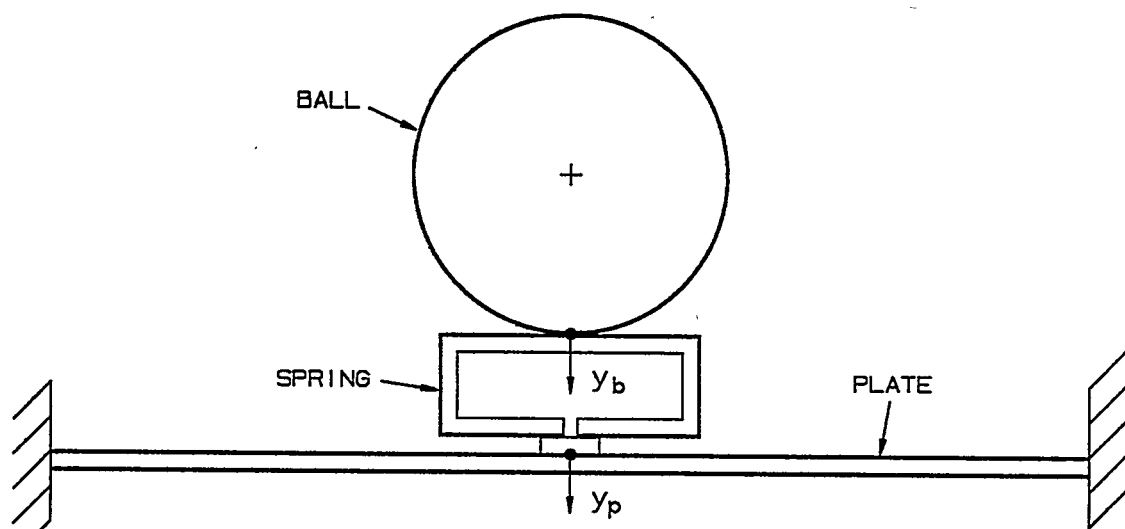
Several short-term PDOs followed, each of which has advanced the understanding of this energy-absorbing device. As a result, we now seem to be in a position where we can evaluate analytically whether this type of device can be made small enough to do a given job in a given volume. An invention disclosure has been filed on the flat plate device.

Many mechanisms involve rotary, rather than linear, motion; and it may not be obvious that a ball dropping onto a flat plate is mechanically equivalent to a rotating arm striking a similar flat plate. This equivalence will be discussed in more detail in Appendix C, and it is the basis for the bulk of the experimental work done on the flat plate device to date.

Zener's article contains three things which are useful in our analysis. He shows that a large thin flat plate has the property that the velocity of the plate in the vicinity of the impact is proportional to the force applied, the same as that shown by viscous damping. He gives an expression for the inverse of that proportionality constant in terms of the plate material and geometry. He also gives an expression that relates the wavelength of a flexural wave in a flat plate to the frequency of the wave. These expressions will be shown later, but with some changes in nomenclature from his article.

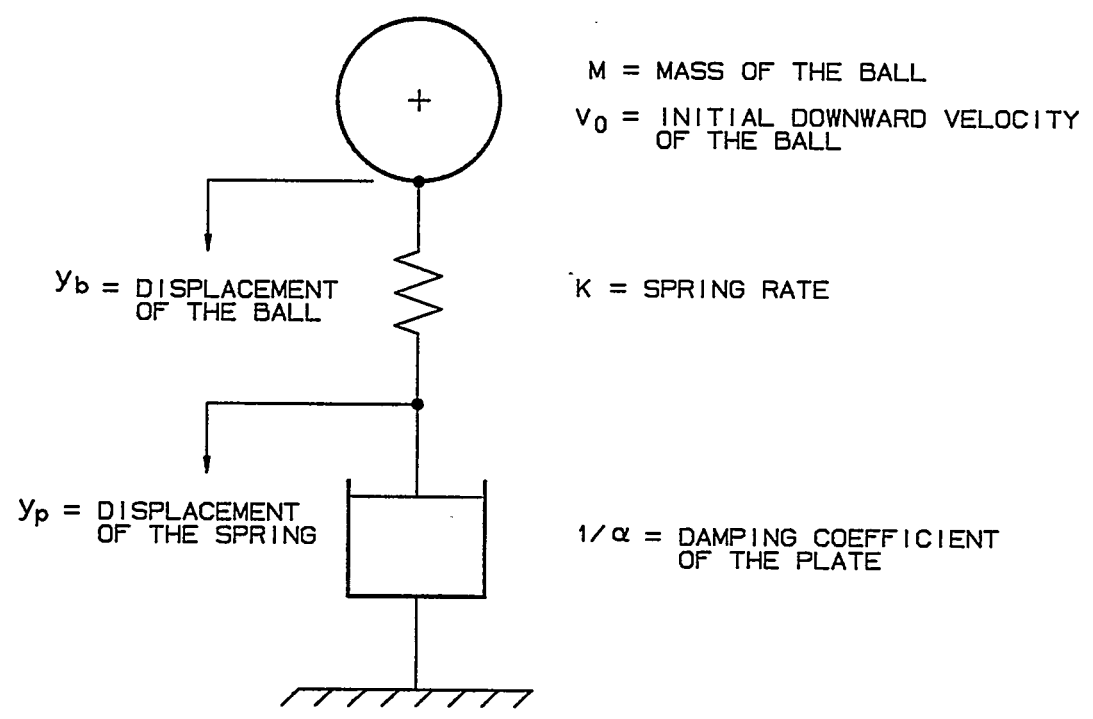
Analysis of Infinite Plate

In Zener's analysis, the sphere and the flat plate are locally deformed due to contact stresses. These deformations serve as a nonlinear spring. We have replaced the nonlinear spring with a linear spring, both to simplify the analysis and to make the spring rate independent of the geometries of the ball and the plate. Figure 1a shows a simplified sketch of the elements of the flat plate device during the time the ball is in contact with the spring. Figure 1b shows a schematic diagram of these elements during the impact process. The plate is shown as a dashpot, since its only significant characteristic is that of a viscous damper. Figure 2 shows a free-body diagram of the three elements involved. The spring is assumed to have negligible mass, so the same force acts on all three elements. We can, therefore, write the following three equations:



y_b = DISPLACEMENT OF THE BALL FROM POSITION AT INITIAL CONTACT
 y_p = DISPLACEMENT OF THE PLATE FROM POSITION AT INITIAL CONTACT

a. SIMPLIFIED SKETCH



b. SCHEMATIC DIAGRAM

Figure 1. Elements of the Flat Plate Device During Impact

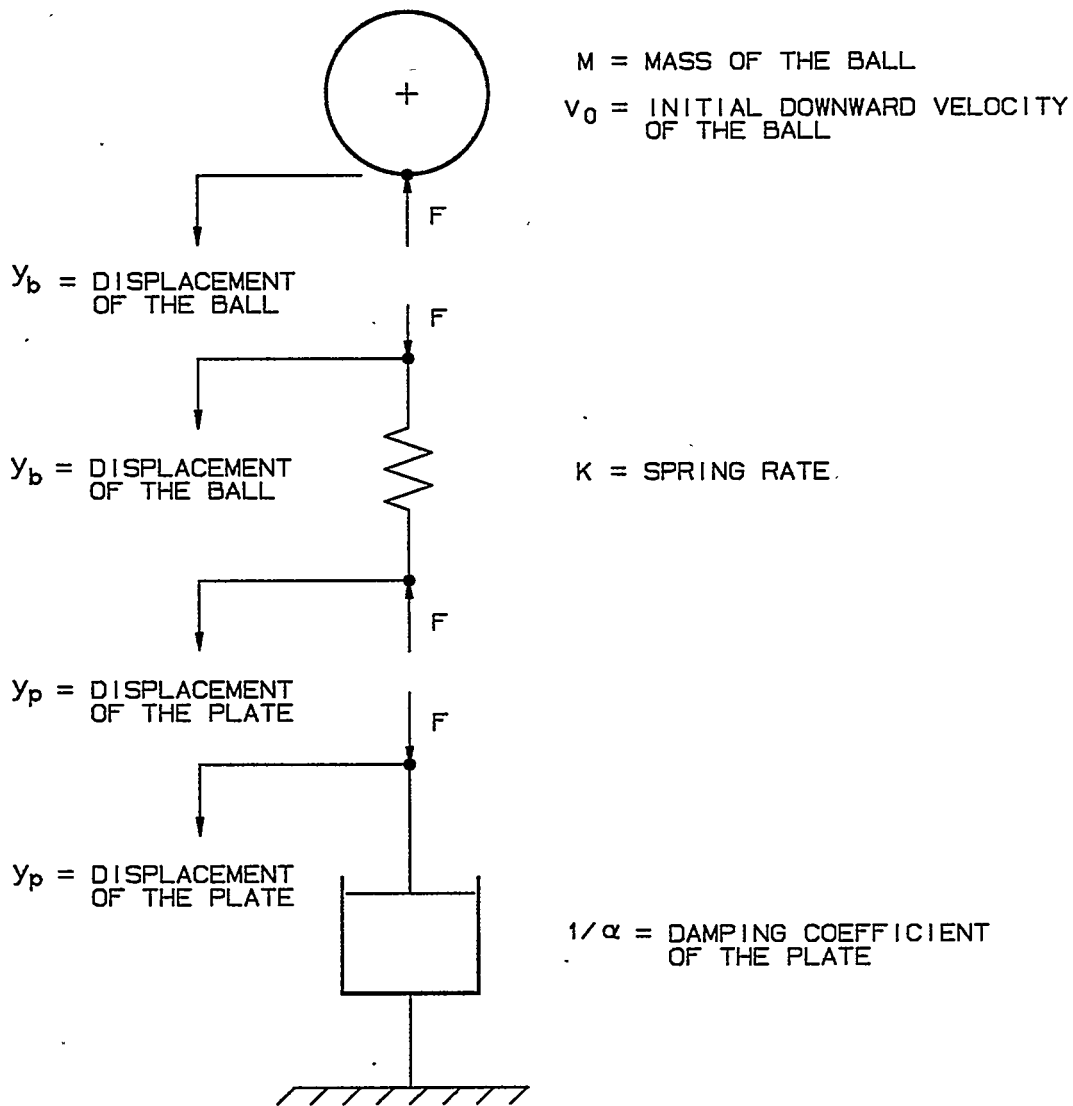


Figure 2. Free-Body Diagram of Elements During Impact

$$F = -M \ddot{y}_b$$

$$F = K (y_b - y_p)$$

$$F = (1/\alpha) \dot{y}_p.$$

Let $x = y_b - y_p =$ deflection of the spring

$$\text{so } \dot{x} = \dot{y}_b - \dot{y}_p,$$

$$\text{and } \ddot{x} = \ddot{y}_b - \ddot{y}_p.$$

$$\text{Then, } (1/\alpha) \dot{y}_p = K x,$$

$$\text{so } \dot{y}_p = K \alpha x,$$

$$\text{and } \ddot{y}_p = K \alpha \dot{x}.$$

$$\text{Also, } K x = -M \ddot{y}_b, \text{ so } \ddot{y}_b = (-K x/M).$$

$$\text{Therefore, } \ddot{x} = \ddot{y}_b - \ddot{y}_p = (-K x/M) - K \alpha \dot{x},$$

$$\text{or } \ddot{x} + (K \alpha) \dot{x} + (K/M) x = 0.$$

J. P. Den Hartog shows how to solve the equation $m \ddot{x} + c \dot{x} + k x = 0$ (Reference 3). The equation was derived for a dashpot in parallel with a spring, both attached between ground and a mass, but we can apply his method of solution to our differential equation, which has the dashpot in series with the spring.

$$\text{Assume } x = e^{st},$$

$$\text{so } \dot{x} = s e^{st},$$

$$\text{and } \ddot{x} = s^2 e^{st}.$$

$$\text{Then, } s^2 e^{st} + (K \alpha) s e^{st} + (K/M) e^{st} = 0,$$

$$\text{or } [s^2 + (K \alpha) s + (K/M)] e^{st} = 0.$$

$$\text{Therefore, } s^2 + (K \alpha) s + (K/M) = 0, \text{ since } e^{st} \neq 0,$$

and

$$s_{1,2} = \frac{-K\alpha \pm \sqrt{(K\alpha)^2 - 4(K/M)}}{2}$$
$$= -\frac{K\alpha}{2} \pm \sqrt{\left(\frac{K\alpha}{2}\right)^2 - \left(\frac{K}{M}\right)}$$

where s_1 is s with the + sign and s_2 is s with the - sign.

Then, the general solution for x is

$$x = C_1 e^{s_1 t} + C_2 e^{s_2 t},$$

where C_1 and C_2 are arbitrary constants which are, in general, complex numbers.

We are interested in the case when $(K\alpha/2)^2$ is less than (K/M) since we want x to return to zero in some finite time. For our case, the expression inside the radical will therefore be negative and we will have to use complex numbers.

A transition in response will occur when the square root term just equals zero, or $(K\alpha/2)^2 = K/M$,

$$\text{or } (K^2 \alpha^2 / 4) = K/M,$$

$$\text{or } 4 = (K^2 \alpha^2 M)/K = K M \alpha^2.$$

Let $\lambda = \sqrt{K M \alpha^2} = \alpha \sqrt{K M}$. The transition in response will then occur when $\lambda = 2$. Since the factor, 2, has no dimensions, λ must also be dimensionless. We can check this by plugging in the dimensions for α , K , and M :

$$\lambda = (\text{in/ lbf sec}) \sqrt{(\text{lbf/in}) (\text{lbf sec}^2/\text{in})} = 1 \text{ (dimensionless).}$$

The units used in this report are discussed in Appendix D.

It will be helpful later to express various quantities in terms of λ , but for now we will continue to use K , M , and α .

Writing the expression for $s_{1,2}$ using complex notation,

$$s_{1,2} = -\frac{K\alpha}{2} \pm j \sqrt{\left(\frac{K}{M}\right) - \left(\frac{K\alpha}{2}\right)^2},$$

where

$$j = \sqrt{-1}.$$

Let

$$q = \sqrt{\left(\frac{K}{M}\right) - \left(\frac{K\alpha}{2}\right)^2}.$$

Then $s_{1,2} = - (K\alpha/2) \pm jq$.

Per Euler's equation, $e^{j\theta} = \cos \theta + j \sin \theta$

and $e^{-j\theta} = e^{j(-\theta)} = \cos(-\theta) + j \sin(-\theta) = \cos(\theta) - j \sin(\theta)$,

so

$$x = C_1 e^{\left(-\frac{K\alpha}{2} + jq\right)t} + C_2 e^{\left(-\frac{K\alpha}{2} - jq\right)t}$$

$$= C_1 e^{-\frac{K\alpha t}{2}} e^{jq t} + C_2 e^{-\frac{K\alpha t}{2}} e^{-jq t}$$

$$= e^{-\frac{K\alpha t}{2}} (C_1 e^{jq t} + C_2 e^{-jq t})$$

$$= e^{-\frac{K\alpha t}{2}} [C_1 (\cos qt + j \sin qt) + C_2 (\cos qt - j \sin qt)]$$

$$= e^{-\frac{K \alpha t}{2}} [(C_1 + C_2) \cos qt + (jC_1 - jC_2) \sin qt].$$

Since C_1 and C_2 are arbitrary constants, $(C_1 + C_2)$ and $(jC_1 - jC_2)$ are also arbitrary constants, so we can let

$$C_1 + C_2 = H$$

and

$$jC_1 - jC_2 = I.$$

Therefore,

$$x = e^{-\frac{K \alpha t}{2}} (H \cos qt + I \sin qt).$$

Now we can apply what we know about the beginning and the end of the impact process. At the beginning, the ball is falling at some velocity, call it v_0 , and the spring hasn't been compressed at all.

So, at $t = 0$: $x = x_0 = 0$, $F = 0$, $\dot{y}_b = \dot{y}_{b0} = v_0$, $\dot{y}_p = 0$, $\ddot{y}_b = \ddot{y}_p = 0$, and

$$\dot{x} = \dot{x}_0 = \dot{y}_b - \dot{y}_p = v_0 - 0 = v_0.$$

We will take the end of the impact process to be the time when the spring is just no longer compressed, so the ball will just be losing contact with the spring. We will call the velocity of the ball at this time v_f .

So, at $t = t_f$: $x = x_f = 0$, $F = 0$, $\dot{y}_b = v_f$, $\dot{y}_p = K \alpha x = K \alpha(0) = 0$, and

$$\dot{x} = \dot{x}_f = \dot{y}_b - \dot{y}_p = v_f - 0 = v_f.$$

We can use these equations to find the constants I and J .

$$x_0 = 0 = e^0 [H \cos(0) + I \sin(0)] = H; \text{ so, } H = 0.$$

Therefore,

$$x = e^{-\frac{K \alpha t}{2}} I \sin qt$$

and

$$\begin{aligned}\dot{x} &= I \left[q e^{-\frac{K\alpha t}{2}} \cos qt + \left(-\frac{K\alpha}{2} e^{-\frac{K\alpha t}{2}} \sin qt \right) \right] \\ &= I e^{-\frac{K\alpha t}{2}} \left(q \cos qt - \frac{K\alpha}{2} \sin qt \right).\end{aligned}$$

So,

$$\dot{x}_0 = I e^0 \left[q \cos(0) - \frac{K\alpha}{2} \sin(0) \right] = I q = v_0,$$

and

$$I = (v_0/q).$$

Therefore,

$$x = \frac{v_0}{q} e^{-\frac{K\alpha t}{2}} \sin qt$$

and

$$\begin{aligned}\dot{x} &= \frac{v_0}{q} e^{-\frac{K\alpha t}{2}} \left(q \cos qt - \frac{K\alpha}{2} \sin qt \right) \\ &= v_0 e^{-\frac{K\alpha t}{2}} \left(\cos qt - \frac{K\alpha}{2q} \sin qt \right)\end{aligned}$$

so

$$x_f = 0 = \frac{v_0}{q} e^{-\frac{K\alpha t_f}{2}} \sin qt_f.$$

Therefore, $\sin qt_f = 0$, since

$$\frac{v_0}{q} e^{-\frac{K\alpha t_f}{2}} \neq 0;$$

so, $qt_f = n$,

and $t_f = n/q$.

Also,

$$\dot{x}_f = v_0 e^{-\frac{K a t_f}{2}} \left(\cos q t_f - \frac{K a}{2 q} \sin q t_f \right)$$

$$= v_0 e^{-\frac{K a \pi}{2 q}} \left(\cos (\pi) - \frac{K a}{2 q} \sin (\pi) \right)$$

$$= v_0 e^{-\frac{K a \pi}{2 q}} (-1 - 0)$$

$$= -v_0 e^{-\frac{K a \pi}{2 q}}$$

$$= v_f.$$

Therefore,

$$v_f = -v_0 e^{-\frac{K a \pi}{2 q}}.$$

We are interested in the final kinetic energy of the ball, as a fraction of its initial kinetic energy.

Therefore, let

$$\eta = \frac{\text{final kinetic energy of the ball}}{\text{initial kinetic energy of the ball}}$$

$$= \frac{1/2 M v_f^2}{1/2 M v_0^2} = \left(\frac{v_f}{v_0} \right)^2 = e^{-\frac{K a \pi}{q}}.$$

Since, in a constant gravity, velocity is proportional to the square root of height,

$$\eta = \frac{\text{bounce height}}{\text{drop height}}$$

= relative bounce height when energy reflected from the edges of the plate is not considered.

The above expression for η can be simplified considerably by introducing the dimensionless variable, λ .

Recall that

$$q = \sqrt{\left(\frac{K}{M}\right) - \left(\frac{K\alpha}{2}\right)^2}$$

and $\lambda = \sqrt{KM\alpha^2} = \alpha \sqrt{KM}$.

Therefore,

$$\begin{aligned} \frac{K\alpha\pi}{q} &= \frac{K\alpha\pi}{\sqrt{(K/M) - (K\alpha/2)^2}} \\ &= \frac{K\alpha\pi}{\sqrt{(K/M)(K\alpha^2/K\alpha^2) - [(K^2\alpha^2)/4]}} \\ &= \frac{K\alpha\pi}{(K\alpha) \sqrt{(1/MK\alpha^2) - (1/4)}} \\ &= \frac{\pi}{\sqrt{(1/\lambda^2) - (1/4)}} \end{aligned}$$

$$= \pi \sqrt{(4\lambda^2)/(4 - \lambda^2)}$$

$$= \frac{2\pi\lambda}{\sqrt{4 - \lambda^2}},$$

a function only of λ .

In order to clean up the expression a little, we can let $\mu = \sqrt{4 - \lambda^2}$.

Then $(K \propto \pi / q) = (2\pi\lambda / \mu)$,

and

$$\eta = e^{-\frac{2\pi\lambda}{\mu}}.$$

We can see that η is a function only of λ , so λ is obviously an important parameter in the problem. We can therefore eliminate one of the other parameters. The best candidate for elimination seems to be the spring constant, K . We can rather freely select any value for the spring constant in order to get the desired value for λ , given the values of M and α . From the definition of λ , we can see that $K = \lambda^2 / (M \alpha^2)$. We will use this expression to eliminate K from our equations. We will also eliminate q , except where it is multiplied by a time variable: $(K \propto \pi / q) = (2\pi\lambda / \mu)$,

$$\text{so } q = (K \alpha \mu) / 2\lambda$$

$$= (\lambda^2 / M \alpha^2) (\alpha \mu / 2\lambda)$$

$$= (\lambda \mu) / (2 M \alpha)$$

$$(K \alpha) / 2 = (\lambda q) / \mu$$

$$\text{and } (K \alpha) / 2q = (\lambda / \mu).$$

Therefore,

$$x = \frac{v_0}{q} e^{-\frac{K\alpha t}{2}} \sin qt$$

$$= \frac{2 M \alpha v_0}{\lambda \mu} e^{-\frac{\lambda q t}{\mu}} \sin q t,$$

and

$$\begin{aligned} \dot{x} &= v_0 e^{-\frac{K \alpha t}{2}} [\cos q t - (K \alpha / 2 q) \sin q t] \\ &= v_0 e^{-\frac{\lambda q t}{\mu}} [\cos q t - (\lambda / \mu) \sin q t]. \end{aligned}$$

There are two more quantities that we should be able to calculate in order to design an actual flat plate device, the maximum deflections of the spring and the flat plate, in order to ensure that they don't bottom out against something. The spring deflection will also give us the force, since we must know the spring rate in order to work the problem.

First, we will find the time, t_x , at which the spring deflection, x , is a maximum, which means that we must set the derivative of x with respect to time equal to zero:

$$\dot{x} = 0 = v_0 e^{-\frac{\lambda q t_x}{\mu}} [\cos q t_x - (\lambda / \mu) \sin q t_x].$$

This requires that $\cos q t_x = (\lambda / \mu) \sin q t_x$,

since

$$v_0 e^{-\frac{\lambda q t_x}{\mu}} \neq 0.$$

So, $\tan q t_x = (\mu / \lambda)$,

$q t_x = \tan^{-1} (\mu / \lambda)$,

or $t_x = (1/q) \tan^{-1} (\mu / \lambda)$.

Also,

$$\begin{aligned} \sin qt_x &= \frac{\tan qt_x}{\sqrt{1 + \tan^2 qt_x}} \\ &= \frac{1}{\sqrt{\frac{1}{\tan^2 qt_x} + 1}} \\ &= \frac{1}{\sqrt{(\lambda^2/\mu^2) + 1}} \\ &= \frac{\mu}{\sqrt{\lambda^2 + \mu^2}} \\ &= \frac{\mu}{\sqrt{\lambda^2 + 4 - \lambda^2}} \\ &= \frac{\mu}{2}. \end{aligned}$$

Therefore,

$$\begin{aligned} x_x &= \frac{2M\alpha v_0}{\lambda\mu} e^{-\frac{\lambda qt_x}{\mu}} \sin qt_x \\ &= \frac{2M\alpha v_0}{\lambda\mu} \frac{\mu}{2} e^{-\frac{\lambda qt_x}{\mu}} \end{aligned}$$

$$= \frac{M \alpha v_0}{\lambda} e^{-\frac{\lambda q t x}{\mu}}$$

and $F_x =$ maximum force applied in the impact process

$$= K x_x$$

$$= \frac{\lambda^2}{M \alpha^2} = \frac{M \alpha v_0}{\lambda} e^{-\frac{\lambda q t x}{\mu}}$$

$$= \frac{\lambda v_0}{\alpha} e^{-\frac{\lambda q t x}{\mu}}$$

To find the maximum plate deflection, y_{px} , we note that $\dot{y}_p = \alpha F = \alpha K x$. Thus, the time derivative of the plate deflection goes to zero when the spring deflection, x , goes to zero, which is at the end of the impact process at the time, t_f . We will have to integrate x over the entire contact duration to find y_{px} .

$$y_p = \int_0^t \dot{y}_p dt$$

$$= \alpha K \int_0^t x dt$$

$$= \alpha \frac{\lambda^2}{M \alpha^2} \int_0^t \frac{2 M \alpha v_0}{\lambda \mu} e^{-\frac{\lambda q t}{\mu}} \sin q t dt$$

$$= \frac{2 \lambda v_0}{\mu} \int_0^t e^{-\frac{\lambda q t}{\mu}} \sin q t dt.$$

From a standard table of integrals:⁴

$$\int e^{ax} [\sin(bx)] dx = \frac{e^{ax} [a \sin(bx) - b \cos(bx)]}{a^2 + b^2}$$

So, $a = -(\lambda q)/\mu$, $b = q$, and $x = t$.

Therefore,

$$\int_0^t e^{-\frac{\lambda q t}{\mu}} \sin qt dt = \left. \frac{e^{-\frac{\lambda q t}{\mu}} \left(-\frac{\lambda q}{\mu} \sin qt - q \cos qt \right)}{\frac{\lambda^2 q^2}{\mu^2} + q^2} \right]_0^t$$

$$= \left. \frac{q e^{-\frac{\lambda q t}{\mu}} \left(-\frac{\lambda}{\mu} \sin qt - \cos qt \right)}{q^2 \left(\frac{\lambda^2}{\mu^2} + 1 \right)} \right]_0^t$$

$$= \left. \frac{e^{-\frac{\lambda q t}{\mu}} \left(-\frac{\lambda}{\mu} \sin qt - \cos qt \right)}{q \left(\frac{\lambda^2}{4 - \lambda^2} + 1 \right)} \right]_0^t$$

$$= \left(\frac{2M\alpha}{\lambda\mu} \right) \left. \frac{e^{-\frac{\lambda q t}{\mu}} \left(-\frac{\lambda}{\mu} \sin qt - \cos qt \right)}{\left(\frac{4}{4 - \lambda^2} \right)} \right]_0^t$$

$$\begin{aligned}
&= \left(\frac{2M\alpha}{\lambda\mu} \right) \left(\frac{\mu^2}{4} \right) e^{-\frac{\lambda qt}{\mu}} \left(-\frac{\lambda}{\mu} \sin qt - \cos qt \right) \Big|_0^t \\
&= \left(\frac{M\alpha\mu}{2\lambda} \right) e^{-\frac{\lambda qt}{\mu}} \left(-\frac{\lambda}{\mu} \sin qt - \cos qt \right) \Big|_0^t
\end{aligned}$$

Therefore,

$$\begin{aligned}
y_p &= \frac{2\lambda v_0}{\mu} \left(\frac{M\alpha\mu}{2\lambda} \right) e^{-\frac{\lambda qt}{\mu}} \left(-\frac{\lambda}{\mu} \sin qt - \cos qt \right) \Big|_0^t \\
&= M\alpha v_0 e^{-\frac{\lambda qt}{\mu}} \left(-\frac{\lambda}{\mu} \sin qt - \cos qt \right) \Big|_0^t \\
&= M\alpha v_0 \left[e^{-\frac{\lambda qt}{\mu}} \left(-\frac{\lambda}{\mu} \sin qt - \cos qt \right) - 1(-0 - 1) \right] \\
&= M\alpha v_0 \left[e^{-\frac{\lambda qt}{\mu}} \left(-\frac{\lambda}{\mu} \sin qt - \cos qt \right) + 1 \right] \\
&= M\alpha v_0 \left[1 - e^{-\frac{\lambda qt}{\mu}} \left(\frac{\lambda}{\mu} \sin qt + \cos qt \right) \right]
\end{aligned}$$

and

$$y_{px} = M\alpha v_0 \left[1 - e^{-\frac{\lambda qt_f}{\mu}} \left(\frac{\lambda}{\mu} \sin qt_f + \cos qt_f \right) \right].$$

Since $t_f = n/q$, then $qt_f = n$,

and

$$\begin{aligned} y_{px} &= M \alpha v_0 \left[1 - e^{-\frac{n\lambda}{\mu}} \left(\frac{\lambda}{\mu} \sin n + \cos n \right) \right] \\ &= M \alpha v_0 \left\{ 1 - e^{-\frac{n\lambda}{\mu}} [0 + (-1)] \right\} \\ &= M \alpha v_0 \left(1 + e^{-\frac{n\lambda}{\mu}} \right). \end{aligned}$$

Since

$$\eta = e^{-\frac{2\pi\lambda}{\mu}},$$

then $y_{px} = M \alpha v_0 (1 + \sqrt{\eta})$.

Note that the expressions for the maximum plate and spring deflections are based on the assumption that there is no energy reflected from the edges of the flat plate. If reflected energy affects the impact, the maximum deflections of the plate and the spring will no doubt be greater than calculated. However, we will see later that we will want to avoid such designs anyway.

Zener's article has an expression for α in terms of the plate material and geometry. Using his equation, our nomenclature, and the definition of the plate modulus, D :

$$\alpha = \frac{1}{4\rho h^2} \sqrt{\frac{3\rho}{E'}} = \sqrt{\frac{3}{16\rho h^4 E'}} = \sqrt{\frac{3}{16\rho h^4} \frac{h^3}{12D}} = \frac{1}{8\sqrt{\rho h D}} = \frac{1}{8\sqrt{mD}},$$

where D = plate modulus,

$$= \frac{E' h^3}{12},$$

h = plate thickness,

$E' = E / (1 - \nu^2)$,

E = modulus of elasticity of the plate material,

ν = Poisson's ratio of the plate material,

ρ = density of the plate material, and

m = mass per unit plan-view area of the plate

= ρh .

Analysis of Finite Plate

In order to account for the energy reflected from the edges of the plate, we will make a number of simplifying assumptions. We will assume that the impact process is unaffected by any reflected energy until time, t_f , when the impact is just over for the infinite plate. We will compute the relative bounce height as discussed for the infinite plate and also a new one for the finite plate and use whichever one gives the greater rebound. We will assume that energy is conserved during the impact process, so any energy lost by the ball, which isn't in the spring, will be in the plate. Therefore, we can compute the energy in the plate at any time in the impact process.

We will show that the flexural wave velocity at which energy is propagated across the plate varies with the wavelength such that the velocity decreases with increasing wavelength. In fact, the velocity will be infinite at a zero wavelength. We will also show that the wavelength will be zero at the beginning of the impact process and will increase with time. We will find the total distance traveled by this wave. This will give us a total travel time for the energy wave to leave the impact point, be reflected one or more times, and arrive back at the impact point. We can think of these flexural waves as continually leaving the impact point. As time goes on, more energy is absorbed by the plate, the wavelength increases, and the wave velocity decreases. There will be some time t_u , during the impact process when the wave can leave the impact point and just get back at the time, t_f , when the impact process will be over. We will assume that the total energy absorbed by the plate up to the time, t_u , will instantaneously become the energy of the ball at time, t_f , with the ball moving in the rebound direction.

Now we will form a new ratio of energies in a form which can be determined from the differential equation we solved. We will use a new symbol, ψ , for this ratio since it is calculated assuming that the energy in the reflected wave is the only thing affecting the impact process. ψ will be the relative bounce height if it is greater than η .

Let

$$\psi = \frac{\text{energy in the plate at time, } t_u}{\text{initial kinetic energy of the ball}}$$

$$= \frac{(U_{b0} - U_{bu}) - U_{su}}{U_{b0}}$$

$$= 1 - \frac{U_{bu}}{U_{b0}} - \frac{U_{su}}{U_{b0}}, \text{ where } U_{b0} = \text{initial kinetic energy of the ball}$$

$$= \frac{M v_0^2}{2}$$

$U_{bu} = \text{kinetic energy of the ball at time, } t_u$

$$= \frac{M \dot{y}_{bu}^2}{2}$$

$\dot{y}_{bu} = \text{first time derivative of } y_b \text{ at time, } t_u$

$U_{su} = \text{potential energy of the spring at time, } t_u$

$$= \frac{K x_u^2}{2}$$

$x_u = \text{deflection of the spring at time } t_u .$

Therefore,

$$\begin{aligned}\Psi &= 1 - \frac{\dot{y}_{bu}^2}{v_0^2} - \frac{K x_u^2}{M v_0^2} \\ &= 1 - \frac{\dot{y}_{bu}^2}{v_0^2} - \frac{\lambda^2}{M \alpha^2} \left(\frac{x_u^2}{M v_0^2} \right) \\ &= 1 - \left(\frac{\dot{y}_{bu}}{v_0} \right)^2 - \left(\frac{\lambda x_u}{M \alpha v_0} \right)^2 .\end{aligned}$$

Now we need to be able to find \dot{y}_b for any given time. Since $\dot{x} = \dot{y}_b - \dot{y}_p$, then,

$$\begin{aligned}\dot{y}_b &= \dot{x} + \dot{y}_p \\ &= v_0 e^{-\frac{\lambda q t}{\mu}} \left(\cos q t - \frac{\lambda}{\mu} \sin q t \right) + K \alpha x \\ &= v_0 e^{-\frac{\lambda q t}{\mu}} \left(\cos q t - \frac{\lambda}{\mu} \sin q t \right) + \frac{\lambda^2}{M \alpha^2} \alpha x \\ &= v_0 e^{-\frac{\lambda q t}{\mu}} \left(\cos q t - \frac{\lambda}{\mu} \sin q t \right) + \frac{\lambda^2}{M \alpha} \frac{2 M \alpha v_0}{\lambda \mu} e^{-\frac{\lambda q t}{\mu}} \sin q t\end{aligned}$$

$$\begin{aligned}
&= v_0 e^{-\frac{\lambda q t}{\mu}} \left(\cos q t - \frac{\lambda}{\mu} \sin q t \right) + \frac{2 \lambda v_0}{\mu} e^{-\frac{\lambda q t}{\mu}} \sin q t \\
&= v_0 e^{-\frac{\lambda q t}{\mu}} \left(\cos q t + \frac{\lambda}{\mu} \sin q t \right).
\end{aligned}$$

Therefore,

$$\frac{\dot{y}_b}{v_0} = e^{-\frac{\lambda q t}{\mu}} \left(\cos q t + \frac{\lambda}{\mu} \sin q t \right)$$

and

$$\frac{\dot{y}_{bu}}{v_0} = e^{-\frac{\lambda q t_u}{\mu}} \left(\cos q t_u + \frac{\lambda}{\mu} \sin q t_u \right).$$

Also,

$$\begin{aligned}
\frac{\lambda x_u}{M \alpha v_0} &= \frac{\lambda}{M \alpha v_0} \frac{2 M \alpha v_0}{\lambda \mu} e^{-\frac{\lambda q t_u}{\mu}} \sin q t_u \\
&= \frac{2}{\mu} e^{-\frac{\lambda q t_u}{\mu}} \sin q t_u.
\end{aligned}$$

Therefore,

$$\begin{aligned}
\psi &= 1 - e^{-\frac{2 \lambda q t_u}{\mu}} \left(\cos q t_u + \frac{\lambda}{\mu} \sin q t_u \right)^2 - \left(\frac{2}{\mu} \right)^2 e^{-\frac{2 \lambda q t_u}{\mu}} \sin^2 q t_u \\
&= 1 - e^{-\frac{2 \lambda q t_u}{\mu}} \left[\left(\cos q t_u + \frac{\lambda}{\mu} \sin q t_u \right)^2 + \left(\frac{2}{\mu} \sin q t_u \right)^2 \right].
\end{aligned}$$

We note that ψ approaches zero as t_u approaches zero.

We must find an estimate for the wave velocity of the flexural wave in the plate. Modifying Zener's expression to use our own nomenclature:

$$\omega = \left(\frac{2\pi}{\Lambda}\right)^2 \sqrt{\frac{D}{h\rho}},$$

where

$$\omega = 2\pi f,$$

f = frequency of a repeating flexural wave, and

Λ = wavelength of a repeating flexural wave.

It may not be obvious at first, but this is an exceedingly powerful equation. It is able to relate the deflection of the center of the plate, as a function of time, to the flexural wave action all over the plate.

For any repeating wave, the period $T = 1/f$

$$= 2\pi/\omega$$

so $\omega = 2\pi/T$.

Substituting for ω in the above expression:

$$\frac{2\pi}{T} = \left(\frac{2\pi}{\Lambda}\right)^2 \sqrt{\frac{D}{h\rho}}$$

$$= \left(\frac{2\pi}{\Lambda}\right)^2 \sqrt{\frac{D}{m}},$$

or

$$\Lambda = \sqrt{2\pi T} \sqrt[4]{\frac{D}{m}}.$$

For an infinite train of sine waves, $\Lambda = c_p T$, where c_p is known as the phase velocity. Unfortunately, we only have part of a single wave and it is only somewhat sinusoidal. Luckily, the mathematicians and physicists have figured out that our wave can be treated as a group of sine waves with frequencies that differ only slightly from each other and that the energy in the group is carried at a group velocity, c_g , which can be fairly easily determined. In the book *Impact*, referenced earlier, we find $c_g = c_p - \Lambda (dc_p/d\Lambda)$.¹ Bringing back our earlier equation for Λ in terms of T , after squaring both sides:

$$\Lambda^2 = 2\pi T \sqrt{\frac{D}{m}} = 2\pi \frac{\Lambda}{c_p} \sqrt{\frac{D}{m}},$$

so,

$$\Lambda = \frac{2\pi}{c_p} \sqrt{\frac{D}{m}},$$

or,

$$c_p = \frac{2\pi}{\Lambda} \sqrt{\frac{D}{m}} = 2\pi \sqrt{\frac{D}{m}} \Lambda^{-1}.$$

Therefore,

$$\frac{dc_p}{d\Lambda} = -2\pi \sqrt{\frac{D}{m}} \Lambda^{-2} = -\frac{2\pi}{\Lambda^2} \sqrt{\frac{D}{m}},$$

and

$$c_g = c_p - \Lambda \left(-\frac{2\pi}{\Lambda^2} \sqrt{\frac{D}{m}} \right) = c_p + \frac{2\pi}{\Lambda} \sqrt{\frac{D}{m}} = c_p + c_p = 2c_p.$$

Therefore,

$$c_g = 2c_p = 2\frac{\Lambda}{T}.$$

We now need some reasonable way to estimate the period of the flexural wave we are concerned about. We can see the general shape of the plate deflection vs time curve by noting that the time derivative of the plate deflection is proportional to the spring deflection, x , which is zero at the beginning and end of the impact process. The plate deflection vs time is therefore an S-shaped curve, as shown in Figure 3. (Figure 3 was actually calculated for the conditions of the medium spring rate.) The inflection point of the curve will be at the time, t_x , when x is a maximum. Up to the inflection point, we could consider the curve to be part of some other curve with a different amplitude. In particular,

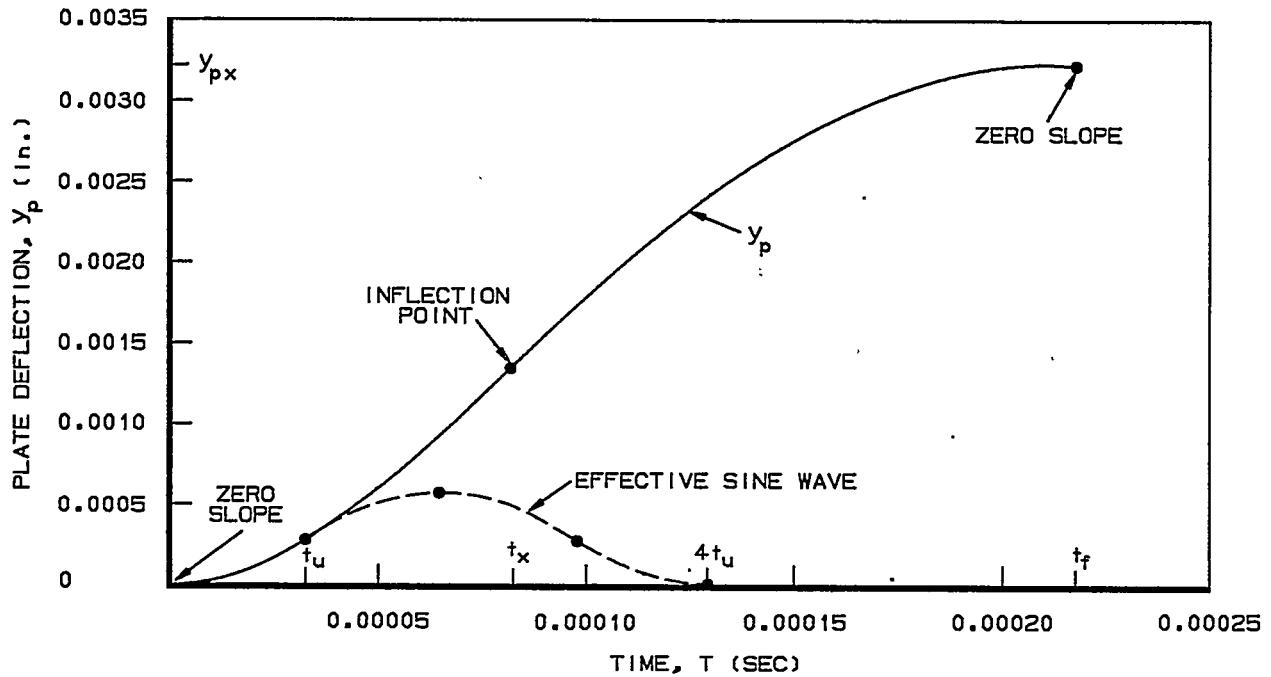


Figure 3. Determination of Effective Sine Wave of Impact

this second curve could be considered to be a sine wave with a period four times as long as the time of contact, t_u , up to that condition. We can consider this to be the effective sine wave of the impact.

Therefore, $T = 4 t_u$,

$$\Lambda = \sqrt{8 \pi t_u} \sqrt[4]{\frac{D}{m}},$$

and

$$c_g = 2 \left(\frac{\Lambda}{4 t_u} \right) = \frac{\Lambda}{2 t_u} = \frac{\sqrt{8 \pi t_u}}{2 t_u} \sqrt[4]{\frac{D}{m}} = \sqrt{\frac{2 \pi}{t_u}} \sqrt[4]{\frac{D}{m}}.$$

We can consider that the last little bit of the energy that we are concerned about is put into the plate at a time, t_u , and will travel with a velocity, c_g . The time available before the end of the impact is $(t_f - t_u)$, so the distance traveled, L_f , by this last little bit of energy is: $L_f = c_g (t_f - t_u)$. When we have found L_f , we will be able to find t_u and then ψ .

We note that the group wave velocity, c_g , increases with decreasing t_u , approaching infinity as t_u approaches zero. This result is obviously erroneous, but we can accept it because it makes our calculations easier and will only make our results somewhat more conservative. We also noted earlier that ψ approaches zero as t_u approaches zero. Thus, we conclude that some small amount of energy always reflects from the edges of the flat plate and affects the impact process. As long as this amount of energy, represented by ψ , is less than that represented by η , we will simply ignore the energy contained in the reflected waves. It might seem that these two energies should be additive, which could double the relative bounce height. It would take considerably more analysis to see which assumption is better, but we will use the first one and compare the theoretical results with the experimental results. We can also note that reflected energy will take some amount of time to be pumped into the ball, but we are conservatively assuming an instantaneous reaction.

We will also make the conservative assumption that the wave will reflect from a straight edge of the plate as if it were reflected from the point nearest the contact point. This will avoid all of the work involved in integrating the energy flow over the included angle of the edge relative to the contact point and also avoid the problem that we don't know how the wave would reflect from an oblique boundary. If all of the edges of a square plate are supported, the waves will return to the contact point when they have traveled a distance equal to the length of one side, half on the way out and half on the way back. In that case, our calculated value for L_f had better not be greater than the length of a side of the plate. However, if two of the sides are supported and two are free, the first return of the waves will essentially cancel and we can allow L_f to be twice as great as the length of a side of the plate, as discussed below.

Sears and Zemansky show schematically the reflections of a single pulse in a taut string from a fixed and from a free end.⁵ They argue that the reflection process can be visualized as an actual pulse and a virtual pulse approaching each other from opposite sides of the end of the string, as shown in Figure 4a. The pulse shapes shown are arbitrary. Where the actual and virtual pulses interact, their displacements are added algebraically. The virtual pulse continues on into the string and becomes a new actual pulse, while the original actual pulse continues on into the virtual extension of the string and we can forget about it. For the fixed end, the displacement of the end of the string must always be zero, so the virtual pulse must be inverted from the actual pulse. Figure 4b shows the pulses after the reflections from the free and the fixed ends, with the pulses now on opposite sides of the string. When they interact at the center of the string, their displacements add to zero, canceling each other out, as shown in Figure 4c. The pulses then continue on to the ends of the string (Figure 4d) and are again reflected (Figure 4e). This time the reflected pulses are on the same side of the string. Now when the pulses interact at the center of the string, their displacements add to double the total displacement (Figure 4f). We can imagine similar pulses, reflections, and cancellations to be set up when a ball impacts a thin flat plate, so the concept of cancellation of first reflections with free and fixed edges seems reasonable, although not proven.

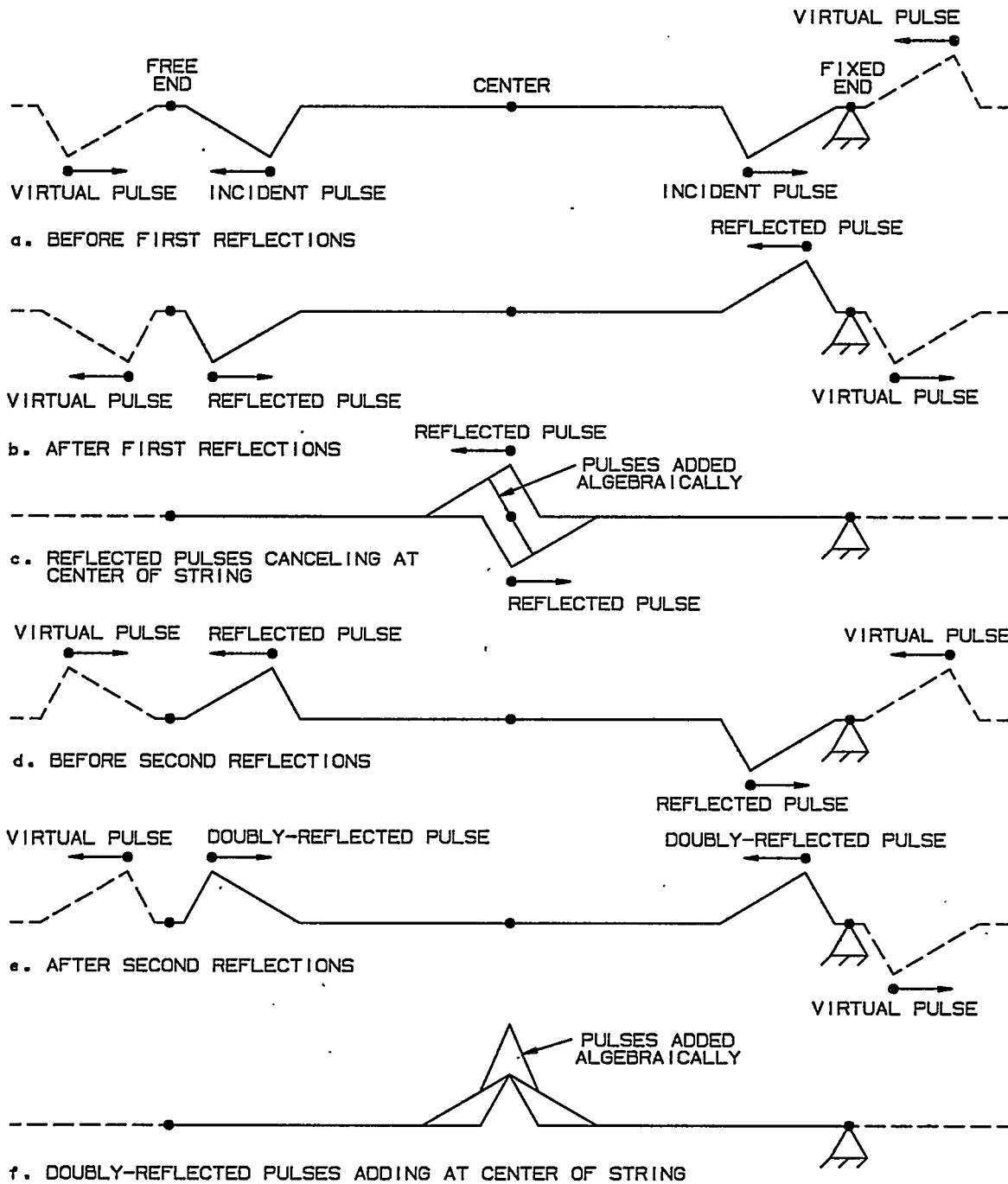


Figure 4. Pulses in a Taut String

If some edges of the flat plate are appreciably further from the impact point than other edges, the wave reflections from the further edges may arrive back at the impact point too late to affect the rebound. We could then modify ψ to account only for the energy reflected from the nearer edges by ratioing it by the included angles. We will ignore that complication and will always take L_f to be equal to twice the length of a side of the square flat plate.

So $L_f = 2 l_s$, where l_s is the length of the side of the square flat plate,

or

$$\begin{aligned} 2 l_s &= c_g (t_f - t_u) = \sqrt{\frac{2 \pi}{t_u}} \sqrt[4]{\frac{D}{m}} (t_f - t_u) \\ &= \sqrt{2 \pi} \sqrt[4]{\frac{D}{m}} \left(\frac{t_f}{\sqrt{t_u}} - \sqrt{t_u} \right). \end{aligned}$$

Therefore,

$$\frac{2 l_s}{\sqrt{2 \pi}} \sqrt[4]{\frac{m}{D}} = \left(\frac{t_f}{\sqrt{t_u}} - \sqrt{t_u} \right).$$

Let

$$\beta = \frac{2 l_s}{\sqrt{2 \pi}} \sqrt[4]{\frac{m}{D}},$$

and

$$y = \sqrt{t_u}.$$

Then

$$\frac{t_f}{y} - y = \beta,$$

or

$$y^2 + \beta y - t_f = 0.$$

So,

$$y = -\frac{\beta}{2} \pm \sqrt{\left(\frac{\beta}{2}\right)^2 + t_f} = -\frac{\beta}{2} + \sqrt{\left(\frac{\beta}{2}\right)^2 + t_f},$$

since γ must be a positive quantity.

Also, $t_u = \gamma^2$.

Thus, for any test condition, we will be able to calculate a value for t_u . The value for t_u will give us a value for ψ :

$$\psi = 1 - e^{-\frac{2\lambda q t_u}{\mu}} \left[\left(\cos q t_u + \frac{\lambda}{\mu} \sin q t_u \right)^2 + \left(\frac{2}{\mu} \sin q t_u \right)^2 \right].$$

We can consider what happens if we make a plate of a given thickness too small in the plan-view dimensions: the plate will no longer be "thin," it will no longer store the input energy in flexural waves, and the plate will no longer act as a viscous damper.

What if we use a laminated plate? Only two pertinent parameters, c_g and α , depend on the properties of the plate. Let's see what happens to these parameters when the plate is laminated.

Assume that the plate is made up of N identical layers, each of thickness, h . Then:

m_i = mass per unit plan-view area of an individual layer,

$$= \rho h,$$

D_i = plate modulus of an individual layer,

$$= \frac{E' h^3}{12},$$

c_{gi} = group velocity of an individual layer,

$$= \sqrt{\frac{2\pi}{t_u}} \sqrt[4]{\frac{D_i}{m_i}},$$

and $\alpha_i = \alpha$ of an individual layer,

$$= \frac{1}{8 \sqrt{m_i D_i}} .$$

It is obvious that the masses per unit plan-view area of the individual layers must be added to get the mass per unit plan-view area of the laminated plate. The plate modulus is similar to the stiffness for a beam, and again the values for the individual layers must be added to get the value for the plate. The group velocities for the individual layers are all equal, so are obviously the same as that of the entire laminated plate. Recalling that $F = (1/\alpha) y_p$, we see that the term $1/\alpha$ acts like a viscous damping coefficient, so the inverses of the α_i terms must be added to get the inverse of α for the plate.

Therefore, we have for the laminated plate:

$$m = N m_i = N \rho h,$$

$$D = N D_i = \frac{N E' h^3}{12} ,$$

$$c_g = c_{g_i} = \sqrt{\frac{2 \pi}{t_u}} \sqrt[4]{\frac{D_i}{m_i}} = \sqrt{\frac{2 \pi}{t_u}} \sqrt[4]{\frac{D/N}{m/N}} = \sqrt{\frac{2 \pi}{t_u}} \sqrt[4]{\frac{D}{m}} ,$$

and

$$\frac{1}{\alpha} = N \frac{1}{\alpha_i}$$

or

$$\alpha = \frac{\alpha_i}{N} = \frac{1}{8 N \sqrt{m_i D_i}} = \frac{1}{8 \sqrt{(N m_i)(N D_i)}} = \frac{1}{8 \sqrt{m D}} .$$

We see that we can write the equations for both c_g and α of the laminated plate in terms of the m and the D of the laminated plate, giving the same equations we had for the single-layer plate earlier. We just have to remember that both m and D now have an N term in them.

For the above equations, we have assumed that each of the individual layers is independent of all of the others. This would not be the case if the layers could touch each other. Not only would there be friction between the layers which would cause mutual moments, but even without friction the layers could not take on their proper shapes. A gap between adjoining layers would allow the outer bend radius of one plate to be larger than the inner bend radius of the adjoining plate. We can estimate the size of the required gap once we have found the maximum deflection of the plate and the wavelength of the flexural wave. Since first reflections of the wave will cancel and second reflections will add, we should double the calculated maximum plate deflection. The gap required has been calculated several ways for typical conditions, and the required gap was found to be only about 0.2% of the thickness of an individual layer of the laminated plate. This value seems to be negligible and the gap can just be sufficient to account for the flatness of the plates. Gaps of 1% to 5% of the thickness of each layer would seem to be adequate.

In precision mechanisms, such as the stronglinks, the gaps will help to prevent the generation of debris, both from the operation of the mechanism and from such environments as mechanical shock and vibration.

When the volume of space available for the flat plate is extremely limited and debris generation is not a major concern, a laminated plate without gaps might be able to be made smaller than one with gaps because of the energy dissipated by the friction. However, variations in the friction coefficient would probably also cause variations in the rebound.

Discussion of Theoretical Results

We will put off a discussion of the theoretical results until we have applied them to the conditions actually tested. At that point, we should be able to tie the various concepts and equations into a coherent picture of the behavior of the flat plate device.

Device Tested

Figure 5 shows a sketch of the flat plate assembly which was tested. Each of the ten layers was 0.0138 in. thick and 1.17 in. on a side, not including the 0.090 in. on each end to act as the fixed-end support. The layers were made of 17-7 PH stainless steel in the annealed condition. The assembly was initially intended to be brazed in such a way that the 17-7 material would end up in the TH1050 hardened condition. In order to speed up the completion of the job, because of the imminent retirement of the author, the assembly was not brazed and the plate material was inadvertently left in the annealed condition. The stresses in the plate must be rather small, since there was no visible damage to the assembly from the testing. The layers were spaced 0.006 in. apart, because that spacer material was available and it was thick enough to be easy to handle. The wedge-shaped pieces at each end allowed the assembly to be held together with friction.

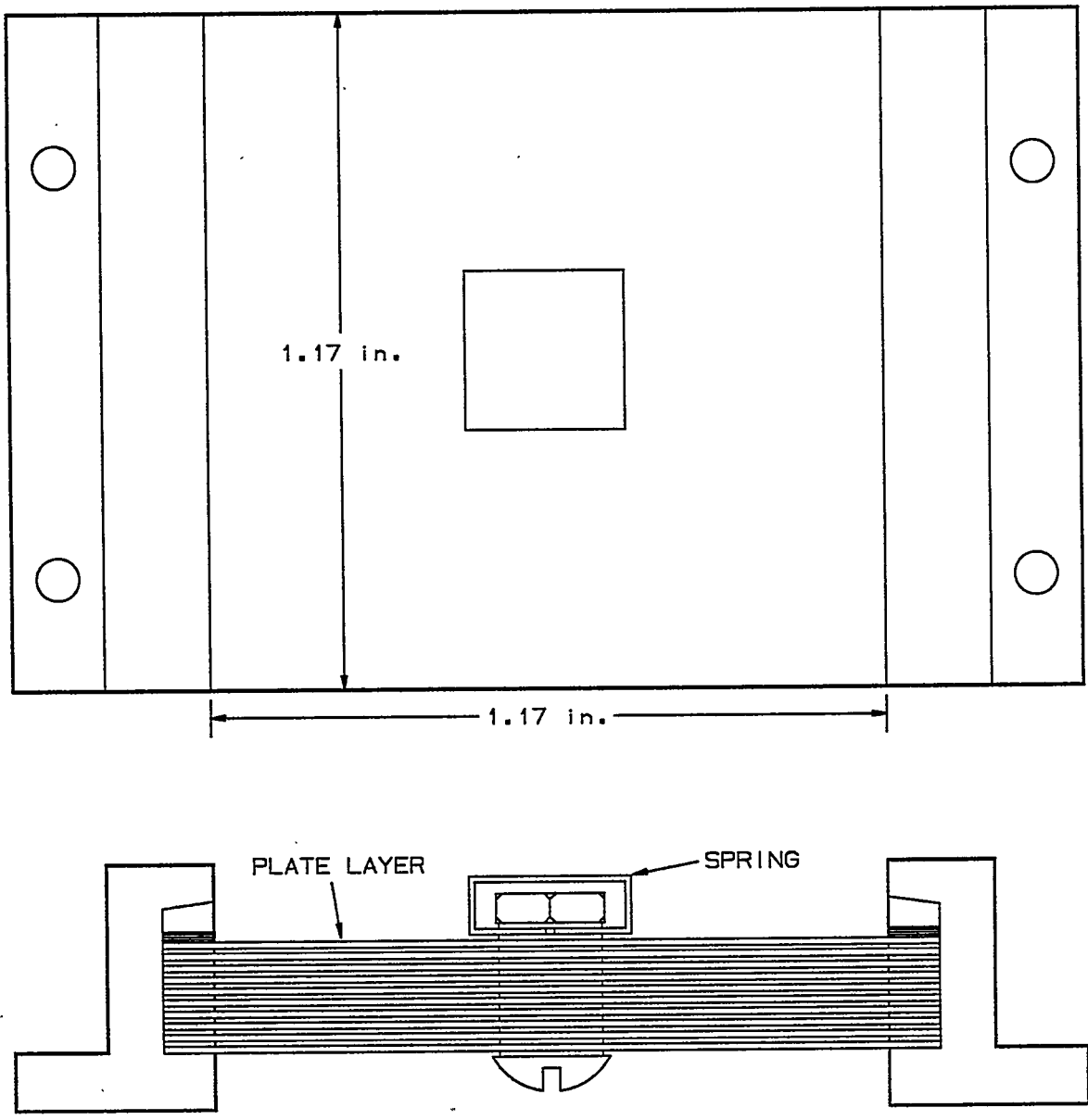


Figure 5. Flat Plate Assembly Tested

The initial box-shaped spring had a theoretical spring rate of 2690 lbf/in., based on an approximate analysis. The spring shape was chosen in order to present a relatively flat surface for the dropping ball to impact and to load the center of the laminated flat plate. The 0.0097-in.-thick spring material was 17-7 PH stainless steel in the TH1050 hardened condition. The spring was 0.265 in. wide, 0.265 in. long as measured from center to center of the vertical walls, and 0.090 in. high from center to center of the horizontal portions.

A second spring of the same type of material had a theoretical spring rate of 10,660 lbf/in. The thickness was increased to 0.0138 in., the length was reduced to 0.222 in., and the height was increased to 0.094 in.

In order to further increase the spring rate, the top free edges of the second spring were rolled over and supported, resulting in the third spring.

The ball to be dropped was held by a vacuum into a shallow inverted cone, centered over the flat plate assembly. The plumbing between the cone and the vacuum pump was partially vented so the ball would release quickly when the vacuum pump was turned off. The cone was a fixed height above the box-shaped spring of the flat plate assembly, so the drop height varied somewhat with the size of the ball. The drop height was taken as

$$h_d = 4.00 - 1.03 d_b,$$

where

h_d = height of the drop, and

d_b = diameter of the ball.

The bounce height was determined from the time between the first and second impacts of the ball with the spring and was taken as

$$h_b = \frac{g}{2} \left(\frac{t_b}{2} \right)^2$$

$$= \frac{g t_b^2}{8}$$

$$= 48.23 t_b^2,$$

where

h_b = height of the bounce,

t_b = time of the bounce, and

g = local acceleration of gravity at the Kansas City Division

= 32.152 ft/sec²

= 385.82 in./sec².

The impacts for the bounce time were measured with an accelerometer, a charge amplifier, and a Visicorder with a chart speed of 40 in./sec. For some of the tests, a high-speed video system with dual cameras was used to ensure that the balls impacted near the center of the spring and that the second impact was with the spring, not the flat plate.

The balls were made of 440C stainless steel material and were available in a range of sizes from 3/32 in. to 1 1/16 in.

Test Results

The spring rates of the box-shaped springs were measured with an Instron load tester. Because the spring rates of the springs were relatively high, the results had to be corrected for the spring rates of the fixture. The corrected spring rates of the springs were taken as

$$K = \frac{1}{\frac{1}{K_{meas}} - \frac{1}{K_{fix}}},$$

where K_{meas} = measured value of the spring rate of the spring and the fixture in series

and K_{fix} = measured value of the spring rate of the fixture only.

The spring rates of the fixture were particularly difficult to measure accurately and had fairly large effects on the corrected spring rates, so the spring rates may be significantly in error. The spring rate results are shown in Table 1.

Table 1. Spring Rate Results

Spring	K_{meas} (lbf/in.)	K_{fix} (lbf/in.)	K (lbf/in.)
#1	1730	12,540	2010
#2	5128	15,170	7750
#3	4656	10,526	8350

The effectiveness of the flat plate assembly in reducing the kinetic energy of the dropped ball is given by the measured relative bounce height, h_{rm} ,

where

$$h_{rm} = \frac{\text{height of the bounce}}{\text{height of the drop}}$$

$$= \frac{h_b}{h_d}$$

The coefficient of restitution is just the square root of the relative bounce height, but doesn't seem to have any particular engineering significance in this problem and has not been computed.

The other significant parameter which is available from the recording of the impacts is the decay time, t_d , for the initial impact. We have arbitrarily chosen to define the decay time as that required for the amplitude of the trace to decay to 10% of its maximum amplitude. If the decay time isn't appreciably less than the bounce time, the plate could have enough residual energy that the second bounce of the ball could be greater than the first bounce. In an actual device, of course, the restoring force for the moving object will not likely be due to the acceleration of gravity so the bounce time will be greatly different from those measured in these experiments, even for the same relative bounce height. In that case, the bounce time would be determined by the kinetics of the system and could be calculated or measured.

The test results are tabulated in Tables 2, 3, and 4 for the low, medium, and high values, respectively, of the spring rate at various ball diameters.

Table 2. Theoretical and Measured Results for Low Spring Rate

	3/32	1/8	5/32	3/16	7/32	1/4	9/32
d_b							
d_b	.09375	.12500	.15625	.18750	.21875	.25000	.28125
M	3.128E-07	7.414E-07	1.448E-06	2.502E-06	3.973E-06	5.931E-06	8.445E-06
λ	.03777	.05815	.08126	.1068	.1346	.1645	.1962
μ	2.000	1.999	1.998	1.997	1.995	1.993	1.990
η	.8881	.8330	.7745	.7146	.6545	.5955	.5382
q	80,149	52,046	37,226	28,302	22,440	18,346	15,353
t_f	3.920E-05	6.036E-05	8.439E-05	1.110E-04	1.400E-04	1.712E-04	2.046E-04
t_x	1.936E-05	2.962E-05	4.110E-05	5.361E-05	6.700E-05	8.113E-05	9.591E-05
h_d	3.903	3.871	3.839	3.807	3.775	3.743	3.710
v_0	54.92	54.70	54.47	54.24	54.01	53.78	53.55
x_k	.0006653	.001004	.001374	.001765	.002170	.002584	.003002
F_x	1.337	2.019	2.761	3.547	4.361	5.193	6.034
y_{px}	.00005026	.0001168	.0002234	.0003772	.0005848	.0008512	.001181
γ	.001175	.001777	.002437	.003142	.003881	.004648	.005438
t_u	1.380E-06	3.158E-06	5.940E-06	9.871E-06	1.506E-05	2.161E-05	2.957E-05
ψ	.00003391	.0001702	.0005737	.001501	.003297	.006368	.01115
c_g	61878	40906	29827	23138	18730	15639	13368
Λ	.1708	.2584	.3543	.4568	.5643	.6758	.791
h_{rm}	.2096	.3363	.4191	.4771	.4947	.4842	.4236
t_d	.0048	.0036	.0037	.0032	.0021	.0041	.0034

K = 2,010

E' = 31,870,000

$\rho = .000715$

h = .0138

N = 10

m = 9.867E-05

D = 69.80

$\alpha = 1.506$

$\beta = .03219$

Table 2 Continued. Theoretical and Measured Results for Low Spring Rate

	5/16	11/32	3/8	7/16	1/2	9/16	5/8
d_b	.31250	.34375	.37500	.43750	.50000	.56250	.62500
M	1.158E-05	1.542E-05	2.002E-05	3.179E-05	4.745E-05	6.756E-05	9.268E-05
λ	.2298	.2652	.3021	.3807	.4652	.5551	.6501
μ	1.987	1.982	1.977	1.963	1.945	1.921	1.891
η	.4834	.4315	.3828	.2957	.2226	.1628	.1154
q	13,085	11,317	9,905	7,806	6,330	5,240	4,404
t_f	2.401E-04	2.776E-04	3.172E-04	4.024E-04	4.963E-04	5.995E-04	7.133E-04
t_x	1.112E-04	1.271E-04	1.433E-04	1.767E-04	2.111E-04	2.461E-04	2.815E-04
h_d	3.678	3.646	3.614	3.549	3.485	3.421	3.356
v_0	53.31	53.08	52.85	52.37	51.90	51.41	50.93
x_x	.003420	.003836	.00425	.005041	.005793	.006495	.007141
F_x	6.875	7.710	8.534	10.132	11.644	13.054	14.354
y_{px}	.001577	.002043	.002579	.003871	.005459	.007343	.009524
γ	.006247	.007071	.007909	.00962	.01139	.01321	.01509
t_u	3.902E-05	5.000E-05	6.256E-05	9.263E-05	1.297E-04	1.744E-04	2.276E-04
ψ	.01809	.02757	.03994	.07432	.1223	.1837	.2573
c_g	11638	10281	9191	7553	6383	5504	4818
Λ	.908	1.028	1.150	1.399	1.656	1.920	2.194
h_{rm}	.3794	.3407	.3401	.2606	.1835	.4364	.6354
t_d	.0032	.0027	.0028	.0030	.0071	.0060	.0053

$K = 2,010$
 $E' = 31,870,000$
 $\rho = .000715$
 $h = .0138$
 $N = 10$
 $m = 9.867E-05$
 $D = 69.80$
 $\alpha = 1.506$
 $\beta = .03219$

Table 2 Continued. Theoretical and Measured Results for Low Spring Rate

	11/16	3/4	13/16	7/8	15/16	1	1 1/16
d_b	.68750	.75000	.81250	.87500	.93750	1.00000	1.06250
M	1.234E-04	1.601E-04	2.036E-04	2.543E-04	3.128E-04	3.796E-04	4.553E-04
λ	.7500	.8546	.9636	1.0769	1.1943	1.3157	1.4410
μ	1.854	1.808	1.753	1.685	1.604	1.506	1.387
η	.07873	.05133	.03160	.01805	.009301	.004135	.001462
q	3.742	3.203	2.753	2.369	2.033	1.733	1.457
t_f	8.395E-04	9.808E-04	1.141E-03	1.326E-03	1.545E-03	1.813E-03	2.156E-03
t_x	3.170E-04	3.526E-04	3.879E-04	4.230E-04	4.578E-04	4.921E-04	5.259E-04
h_d	3.292	3.228	3.163	3.099	3.034	2.970	2.906
v_0	50.44	49.94	49.44	48.94	48.42	47.91	47.39
x_x	.007732	.008267	.008747	.009175	.009553	.009885	.01017
F_x	15.542	16.616	17.581	18.441	19.201	19.868	20.448
y_{px}	.01200	.01478	.01786	.02126	.02501	.02915	.03374
γ	.01705	.01912	.02132	.02372	.02638	.02942	.03305
t_u	2.907E-04	3.654E-04	4.547E-04	5.626E-04	6.959E-04	8.657E-04	1.092E-03
ψ	.3408	.4318	.5273	.6242	.7190	.8079	.8859
c_g	4264	3803	3409	3065	2756	2471	2200
Λ	2.479	2.779	3.100	3.449	3.835	4.278	4.805
h_{rm}	.7419	.6812	.6760	.6834	.7120	.6580	.4810
t_d	.0035	.0028	.0030	.0048	.0032	.0031	.0030

K = 2,010

h = .0138

D = 69.80

E' = 31,870,000

N = 10

 α = 1.506 ρ = .000715

m = 9.867E-05

 β = .03219

Table 3. Theoretical and Measured Results for Medium Spring Rate

d_b	7/32	1/4	9/32	5/16	11/32	3/8	7/16	1/2	9/16
d_b	.21875	.25000	.28125	.31250	.34375	.37500	.43750	.50000	.56250
M	3.973E-06	5.931E-06	8.445E-06	1.158E-05	1.542E-05	2.002E-05	3.179E-05	4.745E-05	6.756E-05
λ	.2643	.3229	.3853	.4513	.5207	.5933	.7476	.9134	1.090
μ	1.982	1.974	1.963	1.948	1.931	1.910	1.855	1.779	1.677
η	.4327	.3577	.2912	.2333	.1837	.1420	.07948	.03973	.01684
q	43,776	35,673	29,726	25,198	21,646	18,791	14,482	11,369	8,980
t_f	7.176E-05	8.807E-05	1.057E-04	1.247E-04	1.451E-04	1.672E-04	2.169E-04	2.763E-04	3.498E-04
t_x	3.285E-05	3.949E-05	4.632E-05	5.331E-05	6.040E-05	6.757E-05	8.201E-05	9.644E-05	1.107E-04
h_d	3.775	3.743	3.710	3.678	3.646	3.614	3.549	3.485	3.421
v_0	54.01	53.78	53.55	53.31	53.08	52.85	52.37	51.90	51.41
x_x	.001010	.001182	.001349	.001510	.001664	.001810	.002078	.002313	.002515
F_x	7.824	9.157	10.45	11.70	12.90	14.03	16.11	17.92	19.49
y_{px}	.0005359	.0007678	.001049	.001380	.001761	.002194	.003215	.004448	.005911
γ	.002093	.002536	.003003	.003494	.004009	.004551	.005722	.007043	.008581
t_u	4.382E-06	6.432E-06	9.018E-06	1.221E-05	1.607E-05	2.071E-05	3.274E-05	4.961E-05	7.363E-05
ψ	.001220	.002531	.004773	.008358	.01379	.02169	.04800	.09522	.1750
c_g	34,727	28,664	24,207	20,806	18,131	15,975	12,705	10,321	8,472
Λ	.3043	.3687	.4366	.5080	.5829	.6616	.8319	1.024	1.248
h_{rm}	.4162	.3414	.2825	.1999	.1555	.1065	.04443	.1476	.3278
t_d	.0049	.0047	.0059	.0059	.0055	.0052	.00590	.0074	.0084

$K = 7,750$ $h = .0138$ $D = 69.80$
 $E' = 31,870,000$ $N = 10$ $\alpha = 1.506$
 $\rho = .000715$ $m = 9.867E-05$ $\beta = .03219$

Table 4. Theoretical and Measured Results for High Spring Rate

	9/32	5/16	11/32	3/8	7/16	1/2
d_b	.28125	.31250	.34375	.37500	.43750	.50000
M	8.445E-06	1.158E-05	1.542E-05	2.002E-05	3.179E-05	4.745E-05
λ	.4000	.4685	.5405	.6158	.7760	.9481
μ	1.960	1.944	1.926	1.903	1.843	1.761
η	.2773	.2201	.1714	.1309	.07099	.03395
q	30,809	26,101	22,405	19,431	14,938	11,680
t_f	1.020E-04	1.204E-04	1.402E-04	1.617E-04	2.103E-04	2.690E-04
t_x	4.445E-05	5.112E-05	5.790E-05	6.473E-05	7.848E-05	9.220E-05
h_d	3.710	3.678	3.646	3.614	3.549	3.485
v_0	53.55	53.31	53.08	52.85	52.37	51.90
x_x	.001288	.001440	.001585	.001722	.001973	.002191
F_x	10.75	12.02	13.23	14.38	16.47	18.29
y_{px}	.001040	.001367	.001743	.002170	.003176	.004393
γ	.002906	.003384	.003887	.004417	.005570	.006884
t_u	8.442E-06	1.145E-05	1.511E-05	1.951E-05	3.102E-05	4.739E-05
ψ	.004546	.008002	.01328	.02102	.04722	.09539
c_g	25,019	21,485	18,703	16,459	13,051	10,560
Λ	.4224	.4919	.5651	.6421	.8098	1.001
h_{rm}	.2175	.1318	.05447	.02872	.1166	.2244
t_d	.0051	.0051	.00670	.00790	.0073	.0073

$K = 8,350$
 $E' = 31,870,000$
 $\rho = .000715$
 $h = .0138$
 $N = 10$
 $m = 9.867E-05$
 $D = 69.80$
 $\alpha = 1.506$
 $\beta = .03219$

Theoretical Results

The equations we developed earlier can be used to find theoretical relative bounce height results for the same conditions as for the test results. We noted earlier that some amount of energy will always be reflected from the edges of the flat plate in time to affect the impact process, but we would ignore that energy until the energy represented by ψ was greater than that represented by η . Also, we will always take L_f to be equal to twice the length of a side of the square flat plate, l_s .

So $2l_s = 2 (1.17 \text{ in.}) = 2.34 \text{ in.}$, and

$$\beta = \frac{2.34}{\sqrt{2\pi}} \sqrt[4]{\frac{m}{D}}$$

We can then find γ , t_u , and ψ .

Earlier equations also give us a value for η at those same test conditions. We then take the relative bounce height, h_b/h_d , to be the greater of η and ψ . These results are also tabulated in Tables 2, 3, and 4 for the three values of the spring rate. η , ψ , and h_{rm} are plotted against ball diameter for the low, medium, and high spring rates, respectively, in Figures 6, 7, and 8.

For these calculations, we have taken the density of the ball as 0.28 lbf/in.^3 , or $0.000725 \text{ lbf sec}^2/\text{in.}^4$,

so $M = 0.0003796 d_b^3 \text{ lbf sec}^2/\text{in.}$

Also $E = 29 \times 10^6 \text{ lbf/in.}^2$ and $\nu = 0.3$, so $E' = 31.87 \times 10^6 \text{ lbf/in.}^2$.

$\rho = 0.276 \text{ lbf/in.}^3 = 0.000715 \text{ lbf sec}^2/\text{in.}^4$.

Discussion of Results

The greatest range of ball sizes was covered with the low spring rate. The results are shown in Figure 6. The curves for η and ψ intersect at a relative bounce height of 0.173 and a ball diameter of about 0.551 in. The minimum measured value for the relative bounce height was 0.1835, at a ball diameter of 0.5000 in., indicating a fairly good theoretical prediction. It doesn't appear to be necessary to double the theoretical relative bounce heights, indicating that the reflected energy is not additive with that energy in the plate which is covered by Zener's theory.

For ball diameters from 0.5 in. down to about 0.25 in., the value for η matches that of h_{rm} rather well; but below that they diverge quickly. For the small ball sizes, the spring itself may act as a thin flat plate, causing a reduced bounce. The data in this region is of only academic interest, since we are trying to predict the behavior of the flat plate device when

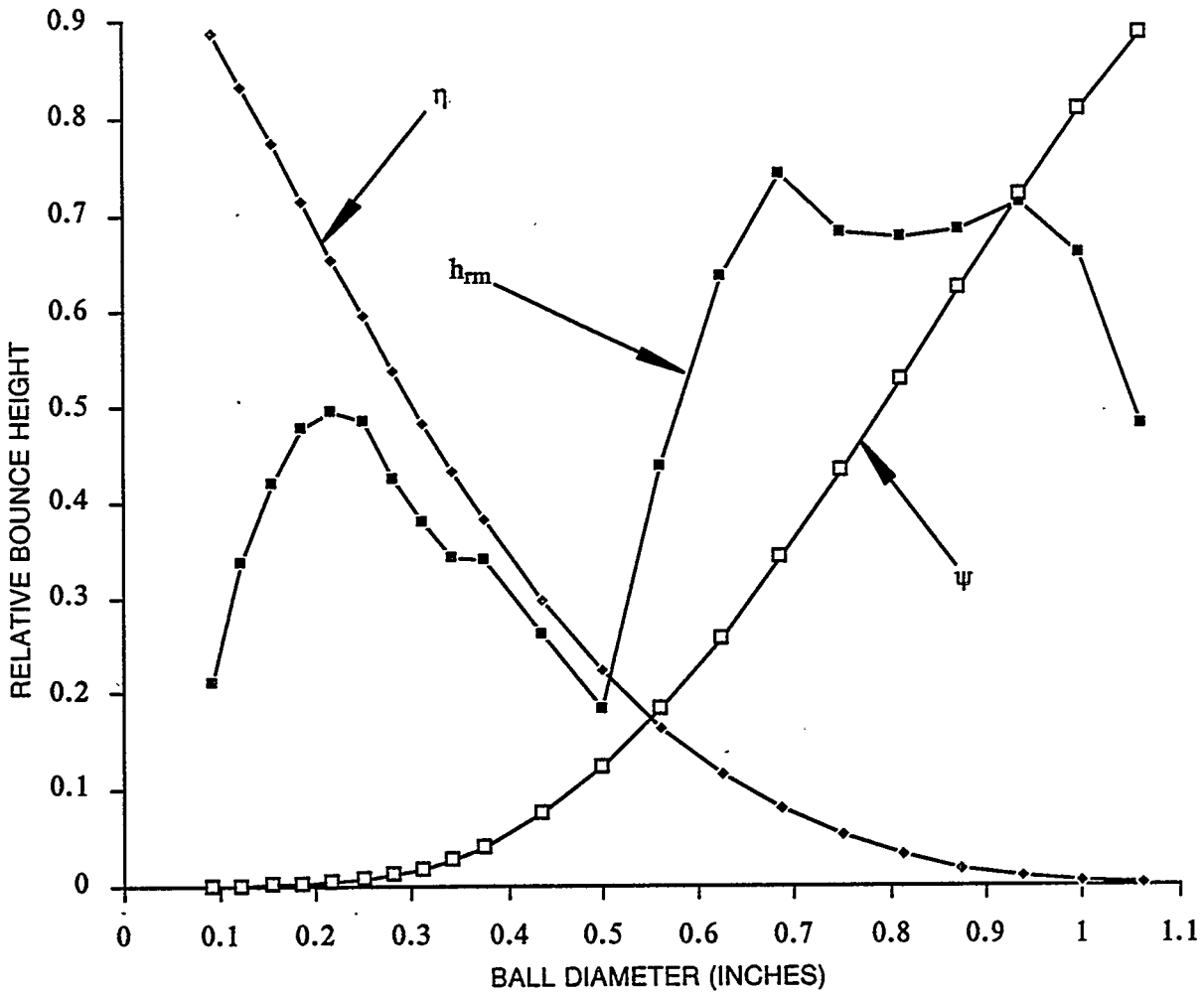


Figure 6. Theoretical and Measured Relative Bounce Heights for Low Spring Rate

the reflected energy is just starting to affect the impact process, in order to minimize the plate size.

For ball diameters from 0.5 in. up to about 0.7 in., h_{rm} increases like ψ , but much faster. This may be because the plate is able to catch up to the rebounding ball, causing an increased bounce. These results warn us to stay out of the region where reflected energy has a significant effect on the impact.

The overall reduction in relative bounce heights for ball diameters above 0.7 in. may be due to localized plastic deformation of the plate material, since it was not hardened, even though there was no evidence of damage to the plate. Also, for diameters of 0.7500 in. and greater, t_u is greater than t_x . Referring to Figure 3, we can see that the effective sine wave of the impact will not be a very good approximation, so our estimate of the energy

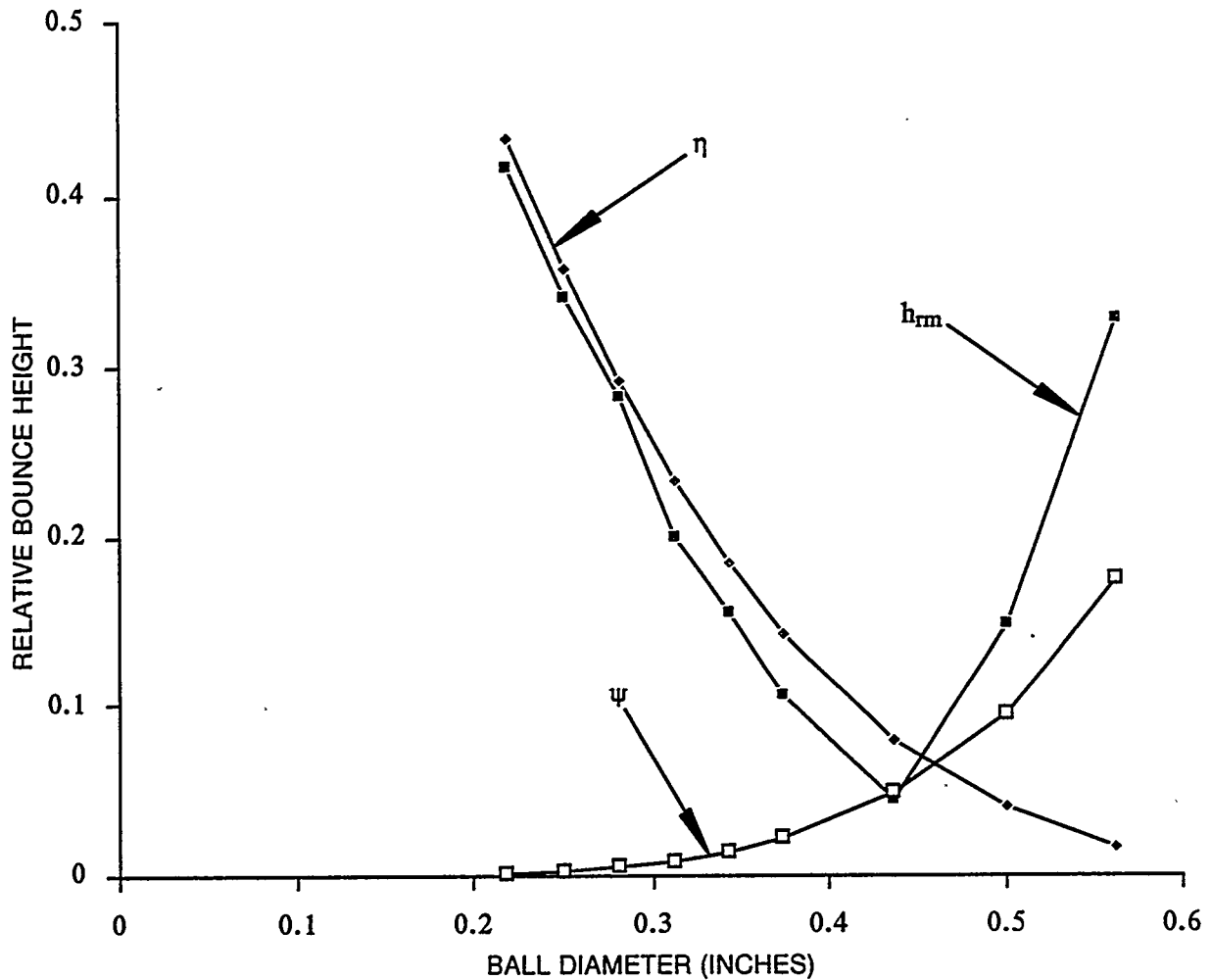


Figure 7. Theoretical and Measured Relative Bounce Heights for Medium Spring Rate

wave velocity will not be very good. The data in this region is interesting but mainly serves to indicate the end of the region of design application.

The results for the medium spring rate are shown in Figure 7. A much smaller range of ball diameter was chosen as the most interesting region for engineering applications. The intersection of the η and ψ curves indicates a minimum relative bounce height of 0.065 at a ball diameter of 0.461 in., compared with the measured minimum of 0.04443 with a 0.4375 in. ball. The overall correlation between theory and experiment seems to be pretty good, although again the measured values increase considerably faster than the theoretical values for the larger balls.

The high spring rate results, shown in Figure 8, show less of a correlation with theory. This may be due to problems in accurately measuring the spring rate of the box-shaped

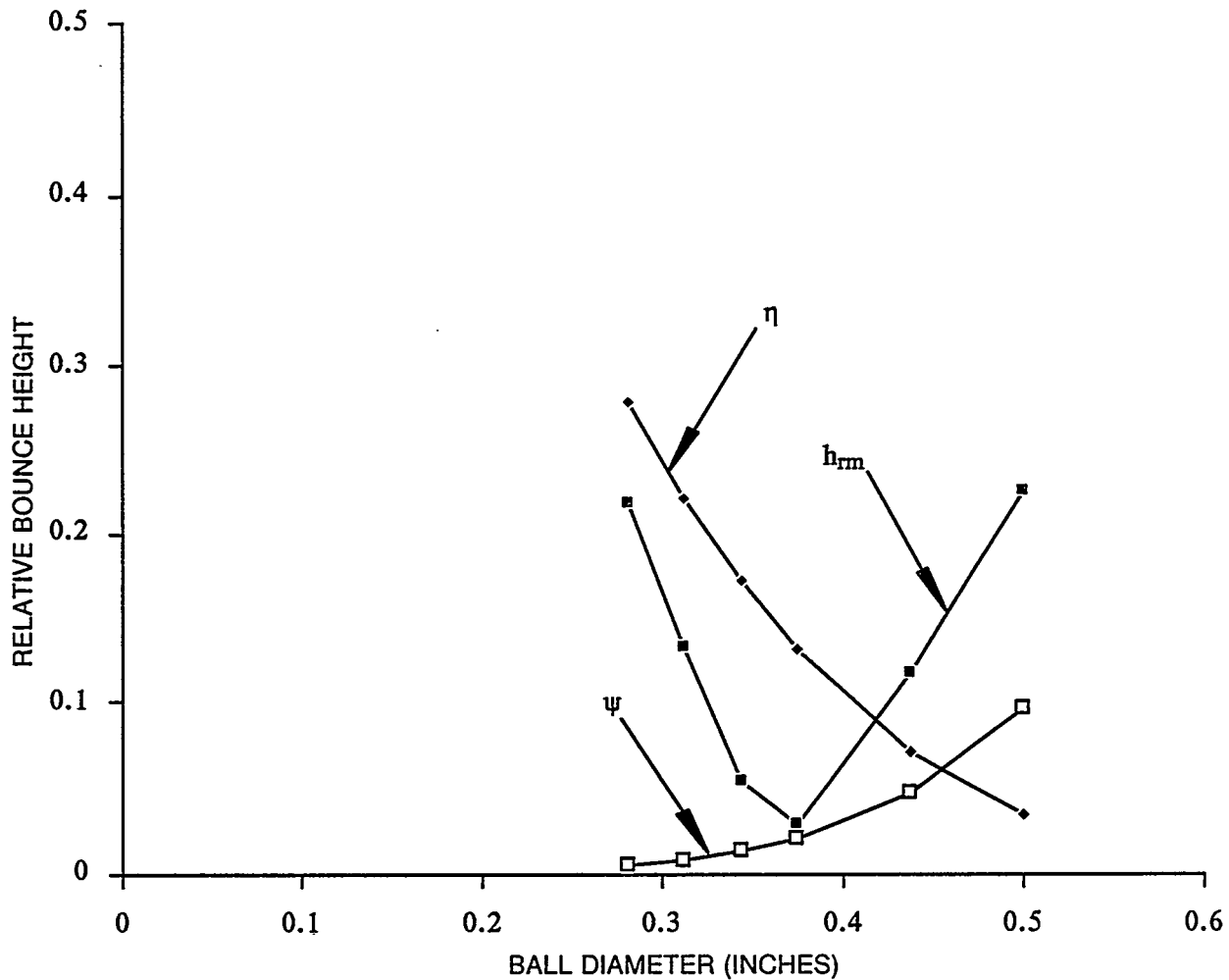


Figure 8. Theoretical and Measured Relative Bounce Heights for High Spring Rate

spring when it is nearly as high as the spring rate of the test fixture, or perhaps even higher.

Predictions From the Theory

The theory we have developed seems to adequately predict the minimum relative bounce height and the ball diameter at which it will occur. We can then use the theory to make some predictions which are inherent in the theory but not obvious from the equations.

The driving force for continuing the development of the flat plate device has been the desire to make it small enough to be useful in miniature mechanisms, such as the stronglinks. We are now ready to predict how small they can get. We will assume a square flat plate and will ignore the small gaps between the laminations when we find the

total thickness of the plate. We will also assume that first reflections from the edges of the plate cancel and the twice-reflected energy wave just arrives back at the impact point at the end of the contact time, so the length of a side of the plate is half of the total distance the energy wave has traveled.

In other words, the minimum relative bounce height will be realized when $\eta = \psi$.

Since

$$\eta = e^{-\frac{2\pi\lambda}{\mu}}$$

and $\mu = \sqrt{4 - \lambda^2}$,

then η is a function only of λ . Therefore, when we select a value for the minimum relative bounce height, we have defined a value for λ , and therefore also for μ . We will not actually solve for λ in terms of η , but it could be done either algebraically or numerically.

Since $\lambda = \alpha \sqrt{KM}$, we can always pick a spring rate, K , for any values of M and α that will give the required value for λ .

We know that $L_f = c_g (t_f - t_u)$,

$$c_g = \sqrt{\frac{2\pi}{t_u}} \sqrt[4]{\frac{D}{m}},$$

and

$$\alpha = \frac{1}{8\sqrt{mD}}.$$

Both c_g and α depend on m and D , but in different ways. We can clarify the analysis by eliminating α , even though it has been useful as an element (which could be interpreted as the inverse of a damping coefficient) and as a shorthand way of referring to the plate properties of m and D .

Expressing the time to the end of the impact process, t_f , in terms of m and D :

$$t_f = \frac{2M\alpha\pi}{\lambda\mu} = \frac{2M\pi}{\lambda\mu(8\sqrt{mD})} = \frac{\pi M}{4\lambda\mu\sqrt{mD}}.$$

ψ is also equal to the minimum relative bounce height and we can use this value to find t_u :

$$\psi = 1 - e^{-\frac{2\lambda q t_u}{\mu}} \left[\left(\cos q t_u + \frac{\lambda}{\mu} \sin q t_u \right)^2 - \left(\frac{2}{\mu} \sin q t_u \right)^2 \right].$$

Since

$$q = \frac{\pi}{t_f} = \frac{4\lambda\mu\sqrt{mD}}{M},$$

we can see that, for a given value of the minimum relative bounce height, t_u depends only on m , D , and M , since λ and μ are already implied. We could numerically determine t_u , but we are more interested in the form of the expression for t_u than in a value.

Therefore, let $\theta_u = q t_u$

so

$$\psi = 1 - e^{-\frac{2\lambda\theta_u}{\mu}} \left[\left(\cos \theta_u + \frac{\lambda}{\mu} \sin \theta_u \right)^2 - \left(\frac{2}{\mu} \sin \theta_u \right)^2 \right].$$

θ_u is then a dimensionless parameter which is completely determined by a value for the minimum relative bounce height, independent of m , D , and M ,

so

$$t_u = \frac{\theta_u}{q} = \frac{\theta_u M}{4\lambda\mu\sqrt{mD}}.$$

Therefore,

$$\begin{aligned} c_g &= \sqrt{\frac{2\pi}{t_u}} \sqrt[4]{\frac{D}{m}} \\ &= \sqrt{2\pi \left(\frac{4\lambda\mu}{\theta_u M} mD \right)} \sqrt[4]{\frac{D}{m}} \end{aligned}$$

$$= \sqrt{\frac{8 \pi \lambda \mu D}{\theta_u M}}$$

Then,

$$\begin{aligned} L_f &= \sqrt{\frac{8 \pi \lambda \mu D}{\theta_u M} \left(\frac{\pi M}{4 \lambda \mu \sqrt{m D}} - \frac{\theta_u M}{4 \lambda \mu \sqrt{m D}} \right)} \\ &= \sqrt{\frac{8 \pi \lambda \mu D}{\theta_u M} \left(\frac{M}{4 \lambda \mu \sqrt{m D}} \right) (\pi - \theta_u)} \\ &= \sqrt{\frac{\pi M}{2 \theta_u \lambda \mu m} (\pi - \theta_u)} \\ &= \sqrt{\frac{\pi}{2 \theta_u \lambda \mu}} (\pi - \theta_u) \sqrt{\frac{M}{m}}, \end{aligned}$$

independent of D.

Let S = plan-view area of the flat plate

$$\begin{aligned} &= \left(\frac{L_f}{2} \right)^2 \\ &= \left(\frac{\pi}{8 \theta_u \lambda \mu} \right) (\pi - \theta_u)^2 \left(\frac{M}{m} \right). \end{aligned}$$

Also let M_p = mass of the flat plate

$$= m S$$

$$= m \left(\frac{\pi}{8 \theta_u \lambda \mu} \right) (\pi - \theta_u)^2 \left(\frac{M}{m} \right)$$

$$= \left(\frac{\pi}{8 \theta_u \lambda \mu} \right) (\pi - \theta_u)^2 M,$$

independent of both m and D !

We can therefore conclude that the mass of the flat plate depends only on the mass of the impacting ball and the chosen value for the minimum relative bounce height.

In most applications the volume, V_p , of the flat plate will be more important than its mass:

$$V_p = \frac{M_p}{\rho}$$

$$= \left(\frac{\pi}{8 \theta_u \lambda \mu} \right) (\pi - \theta_u)^2 \left(\frac{M}{\rho} \right).$$

We can therefore reduce the volume of the flat plate by increasing the density of the flat plate material. Unfortunately, only rather expensive or exotic materials, such as gold and depleted uranium, have densities even twice that of the stainless steels.

There may be a better way to reduce the volume required for the flat plate. The equivalence of the impact of a dropping ball and of a rotating object against the flat plate device is shown in Appendix C. The analysis also shows that a lever can be used to reduce the effective mass of an impacting object, which would also reduce the required volume for the flat plate.

Of course, nothing is ever free, and the effective impact velocity is increased as the effective mass is decreased. The impact velocity directly affects the deflections of the flat plate and the spring, but more importantly affects the stresses in the flat plate. The stresses haven't been analyzed but would certainly increase as the impact velocity is increased. The first indication of a stress problem would probably be fatigue damage to the plate material.

Still, until there is an indication that the design of the flat plate is limited by material stresses, it would be reasonable to use a lever to reduce the required volume for the flat plate and then test for stress problems.

The concept of cancellation of first reflections from the edges of the plate is extended somewhat in Appendix E. The design of a "virtual" pivot for a bellcrank mechanism is also discussed. The bellcrank could turn the impact by 90 degrees, act as a lever to reduce the effective mass of the impacting body, and replace the box-shaped spring.

In Appendix F, dimensional analysis is applied to the flat plate device to show how small devices can be scaled up to larger devices, or vice versa, in order to make them easier to test.

Accomplishments

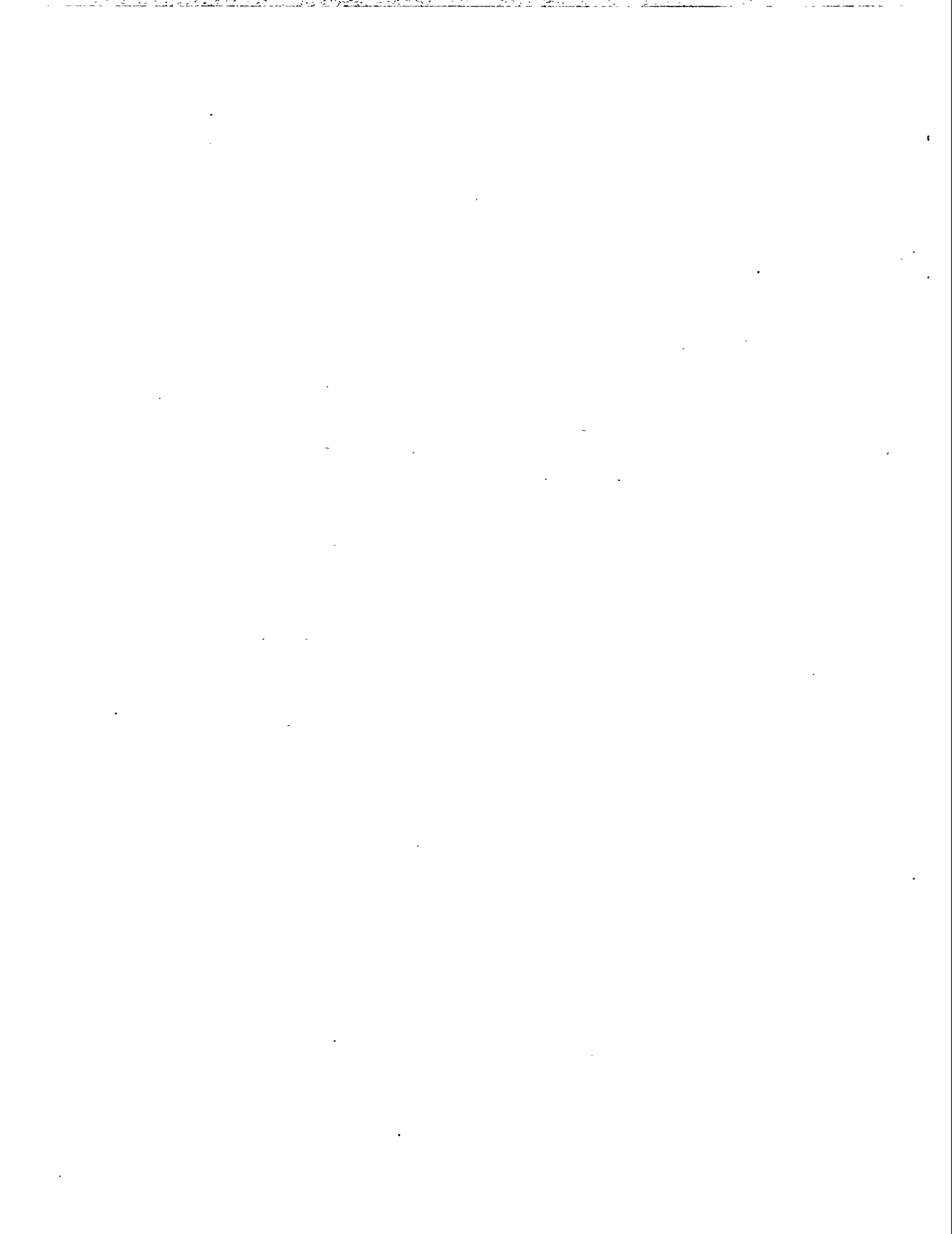
The concepts and analyses presented in this paper should allow the design of a flat plate device for dissipating excess kinetic energy in a given application. However, the stresses produced in the flat plate won't be known so the life of the device will have to be determined by testing.

Future Work

The spring rates for the two available versions of the box-shaped spring should be measured again using a fixture whose spring rate is high enough that it can be ignored.

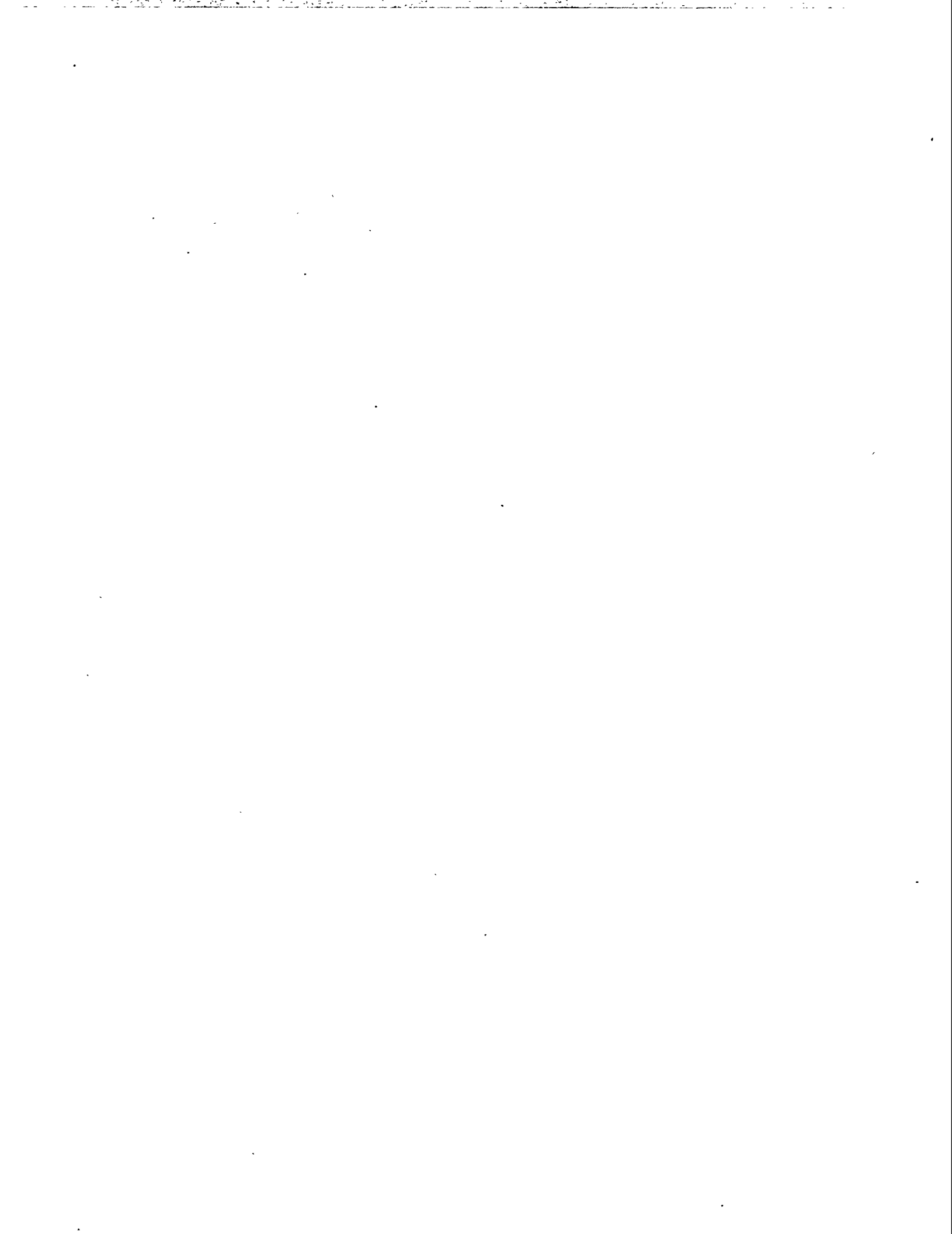
An effort should be made to estimate the stresses produced in the flat plate so the device can be designed to have a good fatigue life.

The assembly should be brazed in order to demonstrate that such a technique is feasible for production.



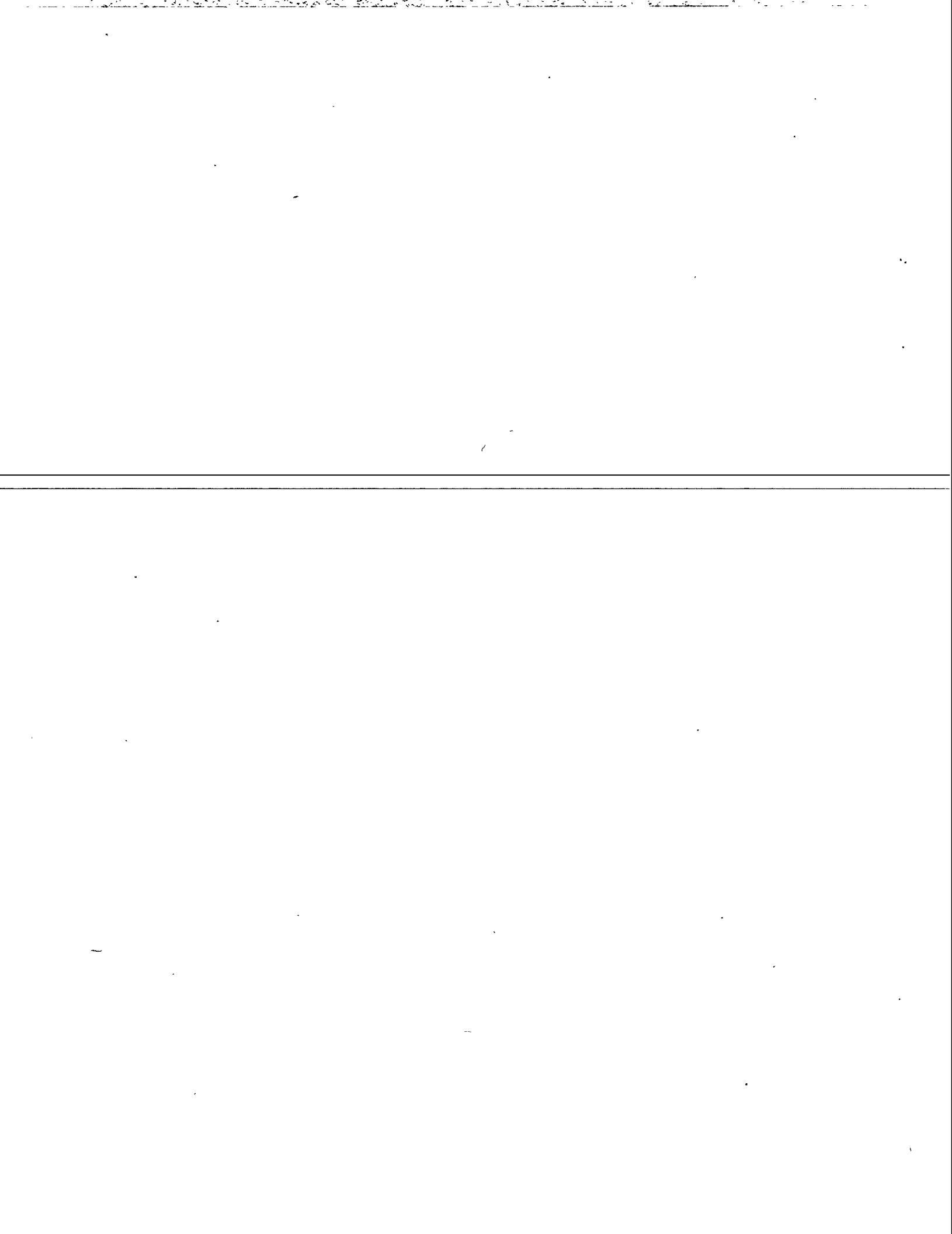
References

- ¹W. Goldsmith, *Impact: The Theory and Physical Behaviour of Colliding Solids*, London: Edward Arnold (publishers) Ltd., 1960, p 30 and p 142.
- ²C. Zener, "The Intrinsic Inelasticity of Large Plates," *Physical Review*, 59, 1941, p 669.
- ³J. P. Den Hartog, *Mechanical Vibrations*, New York: Dover Publications, Inc., 1985, p 37.
- ⁴W. H. Beyer, Ph. D., *CRC Standard Mathematical Tables*, 28th ed., Boca Raton, Florida: CRC Press, Inc., 1987, p 281.
- ⁵F. W. Sears and M. W. Zemansky, *University Physics*, 3rd ed., Reading, Massachusetts: Addison-Wesley Publishing Company, Inc., 1964, p 494.
- ⁶O. W. Eshback, *Handbook of Engineering Fundamentals*, 3rd ed., New York: John Wiley & Sons, 1975, p 426.



Appendix A

Final Report, Thin Flat Plates as Mechanical Stops



FINAL REPORT FOR
STOPS"

"THIN FLAT PLATES AS MECHANICAL

This project had its origin in the observation that a bearing ball, say 1/4" in diameter, would have virtually no bounce, when dropped onto something made of thin metal, such as a desktop address index or an empty in-basket. The observation was both puzzling and exciting. Puzzling because the sheet metal would be expected to act like a spring and return the ball at nearly its impact velocity - not stop it and hold it like a very strong magnet. Exciting because there are so many instances in mechanisms when we would like to kill kinetic energy but just don't have a good way to do it.

At that time, my main concern was the "posigrade cam" redesign. A number of related changes in a return spring, a cam, and a switch rotor would result in a significant improvement in the torque margin available to drive the switch rotor to its enabled position and to return it to its reset position. The big problem, never adequately solved, was in dissipating the kinetic energy of the switch rotor and cam when the return spring drove them back to the reset position. A runaway escapement, similar to another used successfully, was designed into the cam gear. The escapement limited the angular velocity of the cam and rotor during the reset operation to the desired value. However, after only a few operations, the impacting surfaces were greatly peened and abraded. In contrast, the comparable surfaces in the earlier escapement had negligible wear. The big difference between the two designs was that each impact in the posigrade cam redesign had to dissipate much more kinetic energy. In studying the earlier escapement, we were not able to determine how the kinetic energy was dissipated - it just was.

The observed ability of a piece of sheet metal to effectively dissipate all of the kinetic energy of a moving ball seemed to be applicable to the retarding mechanism of the posigrade cam redesign. A book called "Impact" by Werner Goldsmith discussed the very low coefficients of restitution measured when steel spheres were dropped onto thin plates of glass or

metal (pages 142-144). It gave a reference to an article by Clarence Zener (apparently the Zener of the Zener diode) titled "The Intrinsic Inelasticity of Large Plates" as pages 669-673 in Volume 59 of the Physical Review, April 15, 1941. I am constantly amazed by the wealth of information in old (meaning before I got into engineering) articles which isn't easily available to today's engineers. Goldsmith's book, by the way, is an excellent source of such references on the general subject of impacts and nearly all of the references seem to be available at the Linda Hall Technical Library.

Anyway, getting back to Zener's analysis, he derives an equation which indicates that a large, thin flat plate, during an impact, acts like a shock absorber in that the velocity of the plate, near the area where the force is applied, is proportional to the applied force. Of course, under slow loading the deflection of the plate is proportional to the applied force. The Hertzian contact stresses in the area of contact between the sphere and the plate result in a non-linear relationship between the local deformation and the applied force; the applied force is proportional to the three halves power of the local deformation. For the resulting differential equation, which must be solved numerically, Zener shows that the coefficient of restitution depends only on a single dimensionless number he calls the inelasticity parameter, λ . Besides the material properties of density, modulus of elasticity, and Poisson's ratio, λ depends weakly on the impact velocity and is proportional to the square of the ratio of the radius of the sphere to the thickness of the plate. The coefficient of restitution decreases as λ increases.

The coefficient of restitution is often defined as the ratio of the reverse velocity of an object, after an impact, to the forward velocity of the object before the impact. In most mechanism applications, a better parameter is the ratio of final kinetic energy of an object, after an impact, to its initial kinetic energy; therefore to the square of the coefficient of restitution. For an object falling with a constant gravitational acceleration, the ratio of kinetic energies is equal to the ratio of the height of the bounce to the height of the drop. According to Zener's analysis, a

value for λ of 1.0 gives a bounce height which is only 3% of the drop height. For typical engineering materials, such as stainless steel, and typical impact velocities of 100 in/sec, Zener's λ only requires that the plate thickness be less than 20% of the diameter of the impacting sphere. Unfortunately, the whole analysis is based on the assumption that the plate is large enough that the flexural waves set up in the plate can't reflect back from the boundaries in time to affect the impact.

Zener's analysis also allows us to predict the contact time of the impact, which could be coupled with an estimate of a flexural wave velocity to give us an idea of a plate size which would satisfy the requirements of the analysis. His prediction of contact time for the conditions discussed in the previous paragraph is 100 microseconds times the diameter of the sphere.

The only available value for the velocity of a flexural wave having an unknown wave length is the velocity of a Rayleigh wave. The related PDO, "FEA for Flexural Vibration of Beams", may be able to predict wave velocities more accurately. The Rayleigh wave is the maximum possible velocity for a flexural wave in a given material and for normal engineering materials, such as stainless steel, is about 100,000 in/sec. The predicted distance the flexural wave can travel during the contact time is therefore ten times the diameter of the impact sphere. For a circular plate, this would be the diameter of the plate, since the wave would reach the edge of the plate in half that time and just return to the contact point in the other half.

The impacting member of the posigrade cam retarding device was not a sphere, however. It was basically a rectangular bar, pivoted at its center. An equivalent mass can be computed for such a rotating member by dividing its mass moment of inertia by the square of the distance from its center of rotation to its point of impact with the plate. The equivalent mass can then be converted to the diameter of a sphere having a mass equal to the equivalent mass. This computation yielded a diameter of .16" for the equivalent sphere. The angular velocity of the rotating member was

converted to a linear velocity by multiplying by the distance from its center of rotation to the impact point. This linear velocity of 59 in/sec was the equivalent velocity of the equivalent sphere. This velocity could be realized by dropping the sphere from a distance of 4.5". Per Zener's analysis, any plate thickness less than .031" would suffice, but unless the plate could have a diameter of at least 1.55", the theory couldn't predict a small bounce. For plates thinner than .031", the contact time would increase and the plate would probably have to be larger.

Unfortunately, we only had room for a rectangular plate of .3" x .6". It also appeared that a plate .031" thick and .3" wide would not act like a thin plate, but more like an anvil. In order to get some experimental data, it seemed that it might be quicker, cheaper, and more versatile to drop steel balls against thin plates than to try to operate an actual escapement device. There was also the practical problem of measuring something like a coefficient of restitution. By using dropping balls, we could measure the time between the initial impact with the plate and the following impact and compute the bounce height. The coefficient of restitution could be found as the square root of the ratio of the bounce height to the drop height. Actually, the bounce height ratio itself seemed to be more meaningful and was used to evaluate the data. A model 2226C Endevco accelerometer was used to detect the impacts, which were recorded on a model 206 Nicolet digital oscilloscope or a model 1858 Honeywell Visicorder. The latter was preferable as it gave a hard copy of the data, which allowed the decay time of the plate vibration to be determined later.

Another problem was the accuracy with which a .16" ball could be dropped into a .3" x .6" plate. It seemed preferable to drop larger balls onto larger, and thicker plates; then use the theory of dimensional analysis to convert the data back to represent actual sizes. Since the materials of the model balls and plates would be essentially identical to the materials of the actual escapement parts, the dimensional analysis was very straightforward. We had only to note that the velocity of sound, a pertinent parameter to the problem, is a material property, and is therefore the same in the

model and the actual part. The ratio of model times to actual times then had to equal the ratio of model lengths to actual lengths, since velocity is length divided by time. Therefore, the vibration decay times in the actual plate would be less than in the model in the same proportion as the actual length in the plate was to a corresponding model length. The coefficient of restitution, as a ratio of velocities, is already dimensionless and, therefore, the same in the actual device as in the model.

There does seem to be a paradox in the bounce time. We use the bounce time, which must be scaled as the lengths are scaled, to determine the velocity after the first impact, but velocities don't have to be scaled. The resolution to the seeming paradox is the recognition that the bounce time, and also the drop height, are external to the problem. The problem only involves the ball, which has a velocity before impact and a different velocity after impact, and the plate with its supports. The bounce time and the drop height are only used to find the two velocities. Since acceleration is length divided by the square of time, the model acceleration of gravity would have vary as the length ratio divided by the square of the length ratio, or inversely with the length ratio. The moon might then be a good plate to run the tests, if we really cared to include the drop height and the bounce time in the problem. Fortunately, we don't.

A ball-dropping tower was constructed and located on an isolation-mounted table. A ball was supported at one of three heights by means of a vacuum. When the vacuum was relieved, the ball dropped onto a plate. The time of the release was completely unimportant, but any lateral velocity of the ball at the instant of the release would affect the location of the impact point. We therefore went to some effort to get rid of lateral vibrations of the tower.

The tests were successful, in that we were able to find a location on a suitably-sized plate where the bounce height was less than 10% of the drop height. Unfortunately, the patient had died in the meantime. When the posigrade cam redesign effort was ended, the development of the retard

mechanism was also. The plates used in these tests were generally rectangular, with a length twice the width, and made of 304 stainless steel in a cold-worked condition. The variation in the ratio of bounce height to drop height, or relative bounce height, was remarkable. Most plates showed areas where the relative bounce heights were a third of the value at the center of the plate and other areas with three times the value at the center.

The problem of excess kinetic energy in mechanisms is rather general, however. The Dual Stronglink Assembly (DSA), a safety device, also suffers from this malady. In particular, the solenoid and drive arm assemblies of the C module tend to get an extra step of the pattern when the drive arm rebounds from its stop pin. To prevent this behavior, the pattern wheel rotation is damped by preloading the mounting bearings. This is effective, but not entirely desirable. Again, a thin flat plate offered an alternative method for dissipating the excess kinetic energy. Thus, this short term PDO was proposed and authorized.

Whereas the effective diameter of the retard pallet was .16" and there was room for a .3" x .6" plate, that of the C module solenoid and drive arm assembly was .30", and there was only room for a .2" x .6" plate. The allowed shape of the plate wasn't even rectangular, but more of a hollow semicircle. Taking the plate thickness as 20% of the ball diameter, as indicated earlier, gives a plate thickness of .060". A plate .060" thick x .2" wide doesn't seem to fit the requirement of a "thin" plate. Therefore, it seemed likely that the plate would have to be much less than .060" thick.

The tests conducted as part of the present PDO utilized the same ball-dropping tower indicated above. A better X-Y indexing table was purchased in order to improve the positioning of the plates. A variety of 440C stainless steel balls, from 3/32" to 1 1/16" in diameter was also purchased.

The first plates to be tested were made of .031" and .062" thick 17-7 PH stainless steel. The plates had square tops, 15" on a side, hopefully large enough that reflections from

the supports would not affect the impacts. A support was formed by turning an edge down, then out, giving a flange which could be bolted to a much heavier plate. One plate of each thickness had supports on all four sides and one of each thickness had only two opposite sides supported. The plates were heat treated to TH1050 after forming.

For the .062" thick plates and a 3/32" diameter ball, the relative bounce height was .66 with four supports and .69 with two supports vs. a theoretical value of .73. With a 3/16" ball, the respective relative bounce heights dropped to .26 and .24 vs. a theoretical value of .28. With a 3/8" ball, the three values were 0, 0, and .004, respectively. Because of the decay time of the initial impact, relative bounce heights less than .04 couldn't be measured and are reported as zero.

For the .031" thick plates, a 3/32" ball represented the same ratio of plate thickness to ball diameter as a 3/16" ball with the .062" plates. The measured relative bounce heights were .24 for both the two and the four support plates, closely matching the comparable results with the .062" plates. Likewise, the .031" plates with a 3/16" ball gave the same results as the .062" plates with a 3/8" balls, namely, no bounce.

The data from these tests show that Zener's theory on the inelasticity of thin plates is quite accurate. The big problem remaining is to get the plates small enough to be useful in miniature mechanisms. To this end, the tests were continued with larger balls, to see when the relative bounce heights started to increase again. For the largest ball available, 1 1/16" diameter, the relative bounce height remained at zero for the .062" plates. For the .031" plate, with four sides supported, the relative bounce height started to increase with a 5/8" ball and increased to a value of .20 with a 1 1/16" ball. With two sides supported, the bounce started to increase at a 3/4" ball and reached .07 with a 1 1/16" ball. These results deserve a comment, but an explanation isn't available. Using the analogy of a wave travelling along a taut string, it seems that a flexural wave in a flat plate reflects differently from a free edge than

from a fixed or simply supported edge. Consider the center of a square flat plate, which has a free edge and an opposite edge supported, as the center is suddenly deflected downward by one unit of deflection. Consider one wave as it heads for the free edge and another identical wave as it heads for the opposite supported edge. When the wave reaches the free edge, the free edge gets accelerated downwards, which results in another downward-deflected wave travelling in the reverse direction and adding to the deflection of the incoming wave, giving two units of deflection. When the other downward-deflected wave reaches the supported edge, the support will not allow the edge to deflect, so the support applies an upward force on the plate, which results in an upward-deflected wave travelling in the reverse direction and subtracting from the incoming wave, giving a net of zero deflection. When the reflected waves reach the impact point, they each return to one unit of deflection. If we continue to follow the wave reflected from the free edge, it will approach the supported edge with one unit of downward deflection. The support causes the wave to reflect with a net deflection of zero. If we continue to follow the wave reflected from the supported edge, it will approach the free edge with one unit of downward deflection. The wave accelerates the free edge upwards, causing the wave to reflect with a net deflection of zero. The two doubly-reflected waves then approach the contact point, which has one unit of deflection, and try to force the contact point back to zero deflection. Therefore, only every second reflection affects the impact process.

When all four edges are supported, the first reflection acts just like the second reflection of the case above. Therefore, every reflection affects the impact process. The difference in behavior may be significant because of the internal damping of the plate material. When only two edges are supported, each element of the plate is flexed twice as often as when all four edges are supported. This difference in energy dissipation may relate to the lower relative bounce height measured using the 1 1/16" ball. If so, the effect may be exaggerated by using an alloy with a very high damping capacity.

Nitinol, a shape memory alloy, is reported in the literature to have a very high damping capacity. However, there doesn't seem to be much information on the condition of the material when it displays the high damping capacity. An associate has rolled a sample of Nitinol, which we supplied, to .83" x 20" x .017". He will cut it into four equal parts to try various heat treatments to try to obtain the high damping capacity. We will try to utilize this material as part of PDO 70989000, "Dead Mechanism Stop Using Thin Flat Plate".

The next step in our test program was to try smaller square plates, 7.06" on a side, made of both 17-7 PH s.s. and of beryllium copper (Be Cu) Alloy 25, heat treated to condition AT after forming. For these tests, the accelerometer data was recorder on Visicorder paper and the decay time of the initial impact was measured. The decay time was taken as the time required for the acceleration signal to decay to 10% of its maximum value. The decay times for these smaller plates were generally short enough that they didn't interfere with finding the bounce time. Consequently relative bounce heights as low as .002 could be measured.

The Be Cu plates were generally not nearly as flat as the 17-7 plates, apparently getting warped when heat treated. The relative bounce height data for the Be Cu plates averaged more or less the same as the 17-7 plates, but the plots against ball diameter had odd and inconsistent shapes. In one case, an attempt was made to flatten a plate and the resulting data was greatly different from the original data. The decay time data for the Be Cu plates was more consistent and averaged 70% greater than the corresponding 17-7 data. The Be Cu results will not be discussed further.

The relative bounce height data for the smaller 17-7 plates correlated well with that of the larger plates. The analysis of the data is rather complicated and must be reported in detail at a later time. By forming dimensionless ratios and cross-plotting the results, it is apparent that the minimum size for a square plate is realized when the plate thickness just satisfies Zener's requirements for a given relative bounce height and ball diameter. For an actual ball diameter of .30" and a desired relative bounce height of .10, the

required plate would be 2.4" on a side and .075" thick, with two opposite sides supported. This plate, obviously, would be much larger than the .2" x .6" available space.

The decay time data for the smaller 17-7 plates was not analyzed in any detail because of the unfavorable results on plate size. The measured values ranged from 6 to 107 milliseconds.

Another approach was much more successful, and seems to allow part sizes which are applicable to the C module drive arm stop. A virtually foolproof way of stopping a sphere with only a slight bounce is to impact it against a larger, stationary, sphere. Most of the kinetic energy is then transferred to the second sphere. If this energy can be dissipated before the second impact, we have the basis for a simple and effective stop. The thin flat plates we have studied seem to offer a good candidate for supporting the stationary sphere since they seem to dissipate energy quickly.

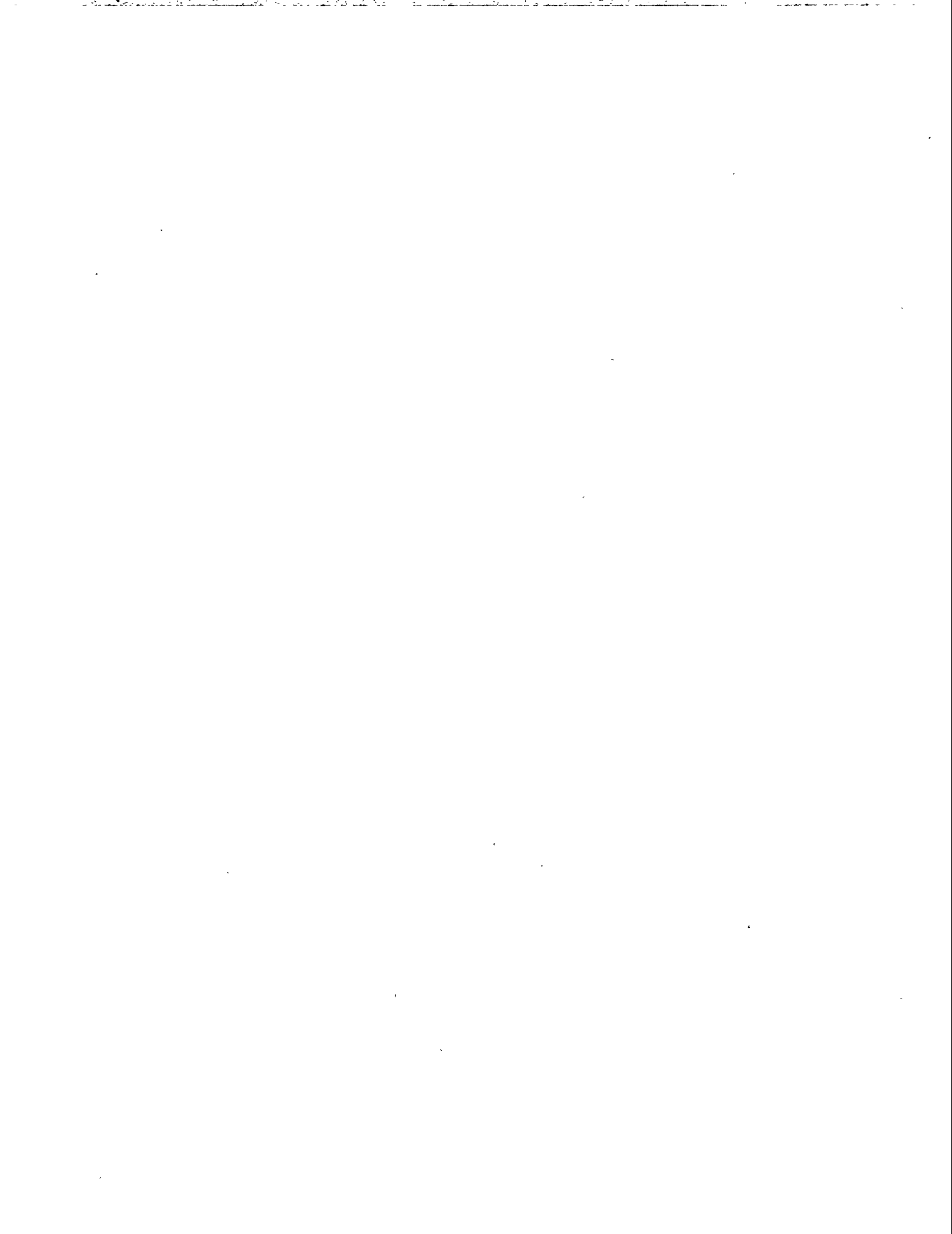
When the stationary sphere is struck, it will take on a simple harmonic motion with the plate acting as the spring. Then, if the reverse velocity of the first sphere after the impact isn't great enough, the second sphere can catch up with it and strike it again. The minimum reverse velocity of the first sphere is realized when this second impact is just avoided. It can be shown that this minimum reverse velocity is 20% of the initial velocity, or a coefficient of restitution of .20. The relative bounce height would be that value squared, or .04, which seems acceptable as a dead stop. This requires that the second sphere have a mass 50% greater than the mass of the first (impacting) sphere.

For test purposes, the second sphere was changed to a cylinder to get a flat surface for the impact and all sizes were scaled up by a factor of three. Thus, a 1" diameter x .729" long cylinder was mounted at the center of a .6" x 1.8" flat plate made of .031" thick 17-7 PH s.s., heat treated to TH1050 and supported by flanges along the .6" wide ends. A .3" diameter x .02" thick washer between the cylinder and the plate was used in order to allow the plate to flex more

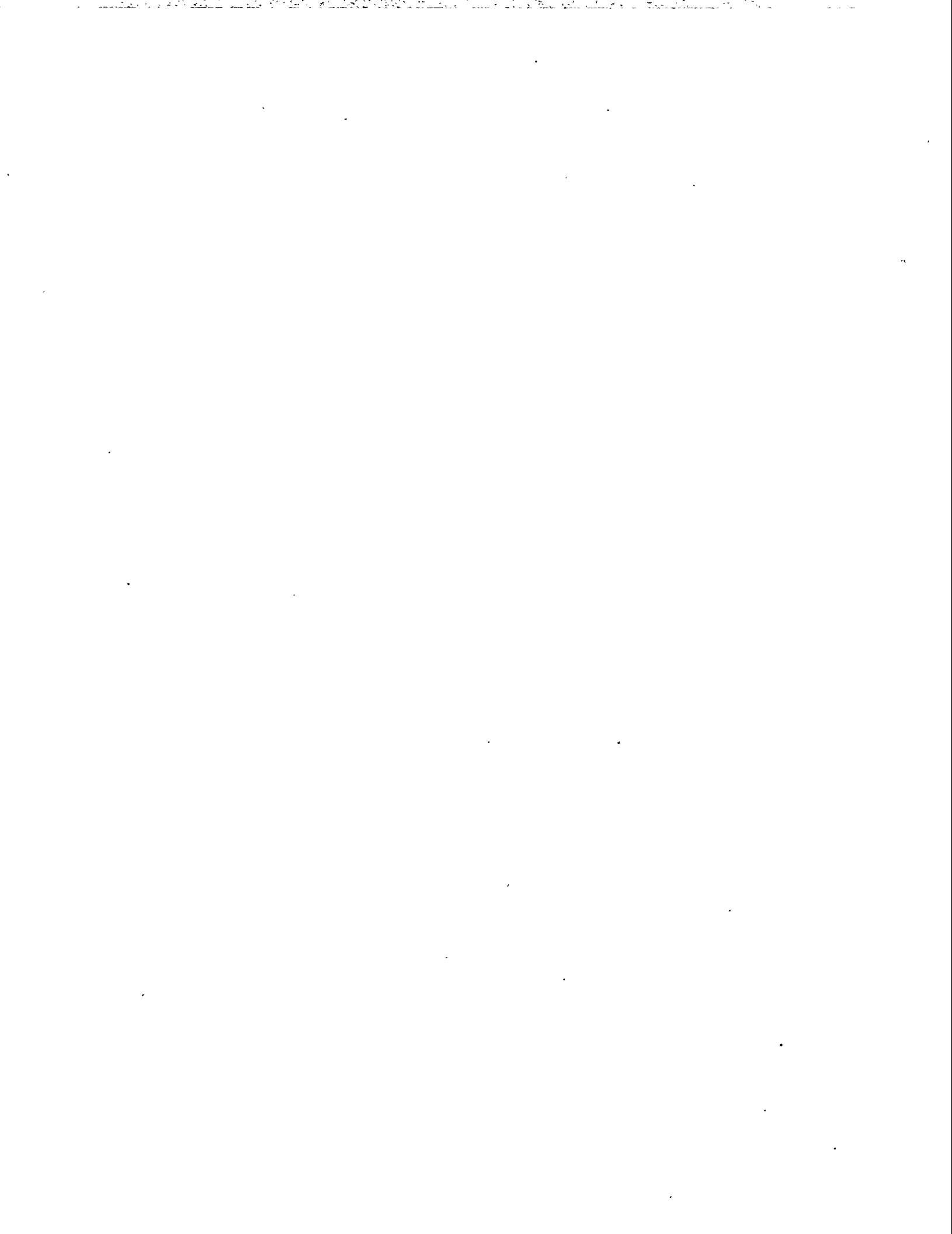
normally. The results of the test were just as expected. A 3:1 scale-up of the .30" diameter sphere wasn't available but 7/8", 13/16", 3/4", and 11/16" balls were tested and the measured relative bounce heights were all within 4% of the predicted values. The relative bounce height for the 7/8" ball was .065 and the decay time was 3.7 ms. When the decay time is scaled down by a factor of three for the actual device, it becomes 1.2 ms.

The cylinder tested, scaled down by a factor of three, becomes .33" in diameter x .24" long, which is too large to be useful. We can, however, strike a pivoted rod near its pivot point to get a large equivalent mass from a small object, as noted earlier. Again using a scale-up by a factor of three, a rod 1.25" long x .193" x .193" was pivoted at .173" from one end. The rod was attached to the center of the .6" x 1.8" plate noted above, at a distance of .97" from the pivot point. The rod was designed to act like a 1" diameter x .729" long cylinder when impacted at .210" from the pivot. When tested, the rod was impacted at .20" and .22", giving values for relative bounce height of .105 and .065 respectively. The measured decay times were 2.5 ms and 3.0 ms, respectively. When the rod is scaled down to actual size, it is .42" long x .064" x .064", which seems to be a reasonable size to fit into an actual unit.

This design appears feasible for an actual mechanism and will be pursued further as "Dead Mechanism Stop Using Thin Flat Plate". Using an alloy with a high damping capacity for the plate may also offer advantages.



Appendix B
Final Report, Dead Mechanism Stop
Using Thin Flat Plate



Final Report for
Thin Flat Plate

Dead Mechanism Stop Using

This PDO is a follow-on to the short term PDO , "Thin Flat Plates as Mechanical Stops." The concepts developed in that earlier PDO were developed further resulting in two dead stop designs. The designs were sized to fit into existing C module mechanisms of the Assembly to act as drive arm stops.

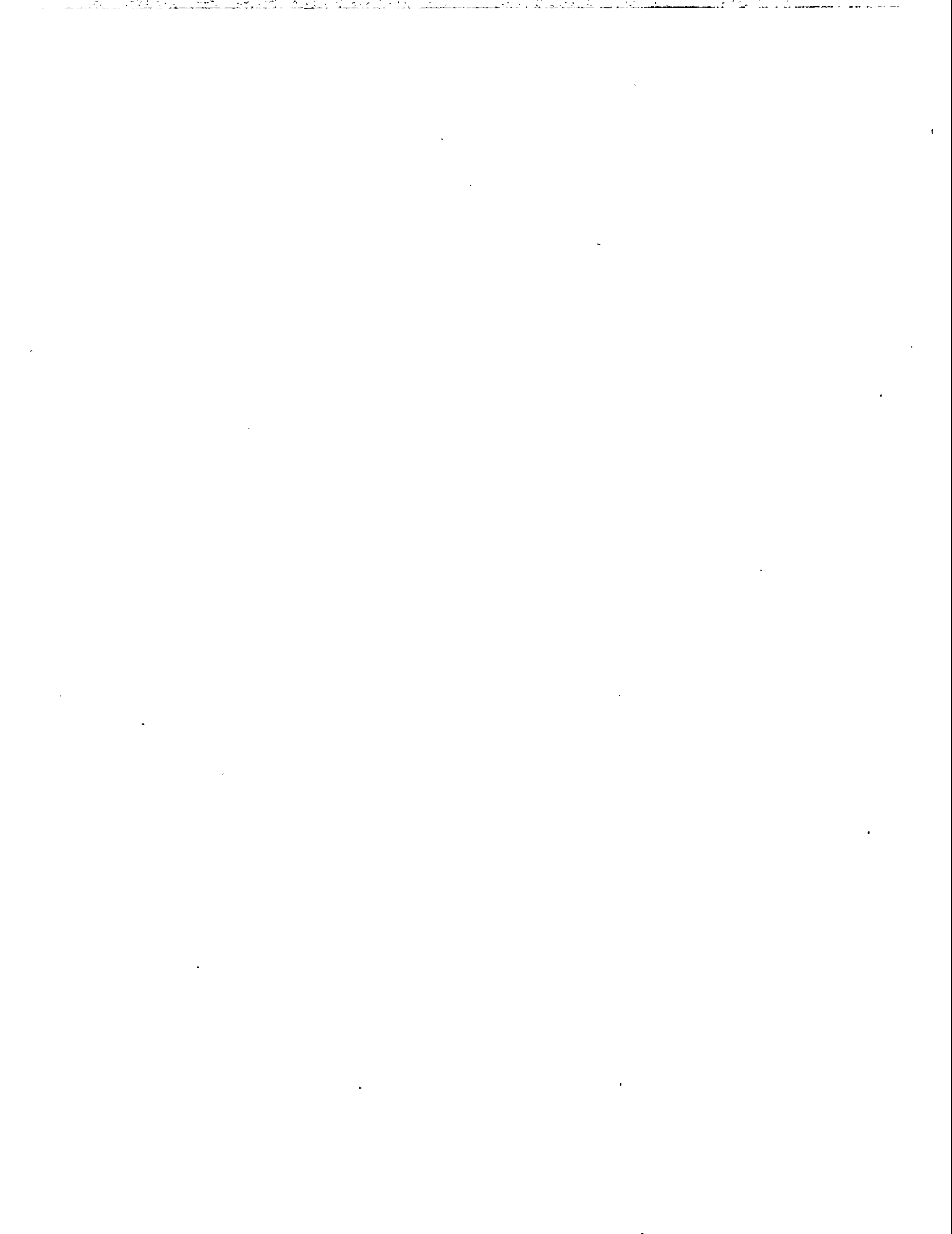
One design was based on a mass and lever assembly which would act as an effective mass just greater than the effective mass of the rotating drive arm and solenoid assembly. The term "effective mass" is used to indicate the mass in a linear motion system which would be equivalent to the mass moment of inertia of the rotational motion system. The required piece parts for this design were fabricated but have not been assembled and tested. In this design, the thin flat plate would only act to dissipate the energy of the impact before the slight rebound of the drive arm would result in a second impact.

The other design utilized a thin flat plate in the sense analyzed by Zener and discussed in the earlier PDO referenced above. This design was actually built and tested. The results were disappointing in that the rebound was essentially identical with that of the normal C module stop pin. Subsequent analysis indicated two problems with the design. The plate was expected to act as a pivot for the part which was contacted by the drive arm, but closer analysis indicated that the plate would not be an effective pivot. The other problem, as indicated by later analysis of the system assuming a linear spring, was that the thin flat plate was too small. This analysis, if supported by testing would be invaluable in determining the properties of the plate and the spring rate of the system to get only a very slight rebound in a given situation. This analysis, coupled with the observation that a rectangular plate with dual impacts could act as if it were simply supported along its midline, indicates that an effective dead stop would fit into the C module.

The concept of a simple, effective, and small dead stop based on Zener's analysis still appears promising. Hopefully, another short term PDO would succeed in demonstrating this promise.

Appendix C

**Equivalence of Impact of Linear and
Rotary Object With Flat Plate**



In order for the impact of a rotary object on a given flat plate device to have the same effect as that of a dropping ball, it seems that three conditions must be met: the impact must be essentially normal, the same three force equations must be satisfied, and the initial condition must be the same. The geometry shown in Figure 1 satisfies the first condition, as long the moment arm, r , is much greater than the maximum value of y_b . In other words, the rotor must move through only a small angle during the impact process.

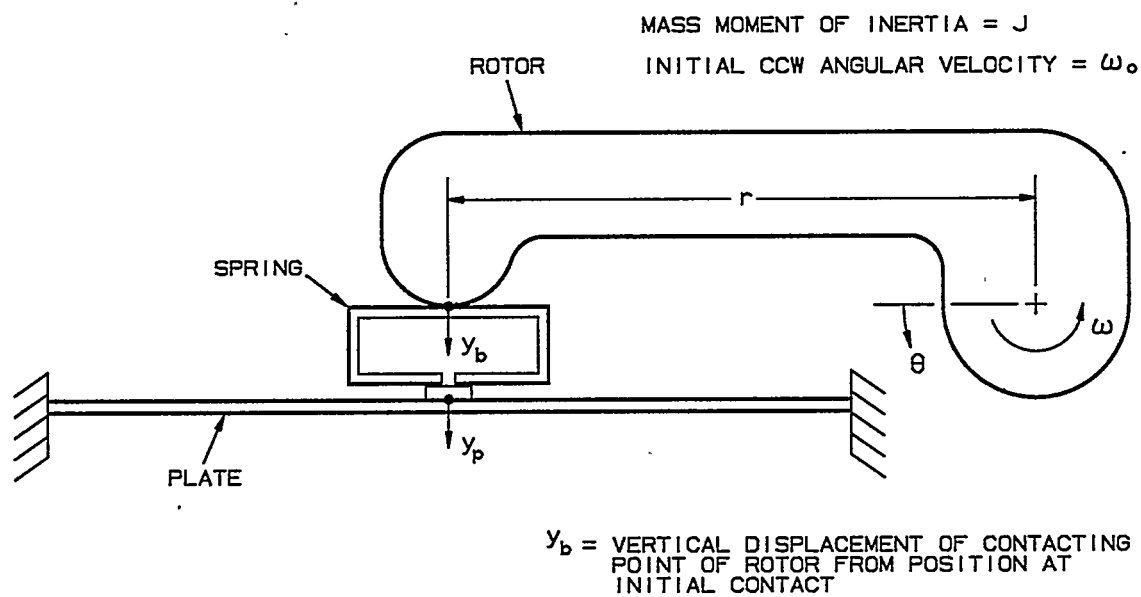


Figure 1. Simplified Sketch With Rotor in Place of Ball

From the geometry, we can see that

$$y_b = r \theta,$$

$$\text{so } \dot{y}_b = r \dot{\theta} = r \omega$$

$$\text{and } \ddot{y}_b = r \ddot{\theta}.$$

We will write the three force equations and the initial condition for the linear and rotary impacts so we can easily compare them:

Impacting ball:

$$F = -M \ddot{y}_b$$

$$F = K (y_b - y_p)$$

$$F = (1/\alpha) \dot{y}_p$$

$$\dot{y}_{b0} = v_0$$

Impacting rotor:

$$F r = -J \ddot{\theta}$$

$$F = - (J \ddot{\theta}/r) = - (J r \ddot{\theta}/r^2) = - (J/r^2) \ddot{y}_b$$

$$F = K (r \theta - y_p) = K (y_b - y_p)$$

$$F = (1/\alpha) \dot{y}_p$$

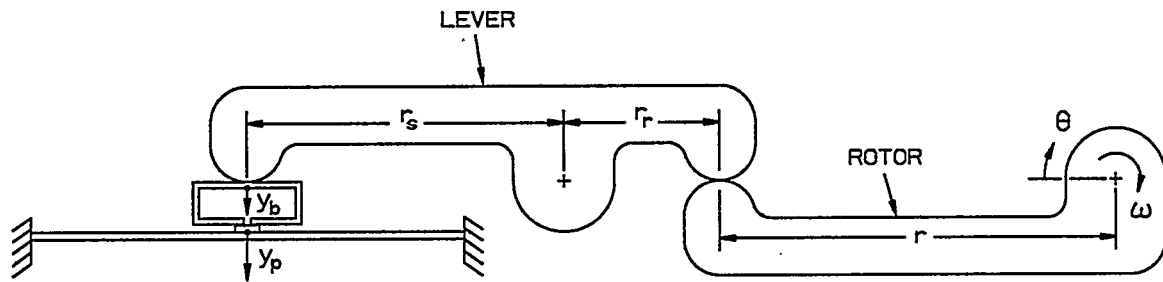
$$r \dot{\theta}_0 = r \omega_0 = \dot{y}_{b0}$$

We see that we can make the two sets of equations identical by setting $J/r^2 = M$ and $r \omega_0 = v_0$. The flat plate device will then respond to the impact of the rotor just as it would to the impact of a ball.

We can think of J/r^2 as an effective mass for the rotor and $r \omega_0$ as its effective velocity (as well as its actual linear velocity). We can also see that increasing the moment arm, r , of the rotor decreases its effective mass and increases its effective velocity. These effects may be useful in reducing the required size of the flat plate.

The effects of increasing the moment arm can be increased by inserting a lever between the impacting object and the spring of the flat plate device. We could analyze the effect of the lever with either an impacting ball or an impacting rotor. We will pick the latter since it is more applicable to miniature mechanisms.

Figure 2 shows such a lever added to the mechanism of Figure 1. From the geometry, we can see that:



y_b = VERTICAL DISPLACEMENT OF CONTACTING POINT OF LEVER WITH SPRING, FROM POSITION AT INITIAL CONTACT

Figure 2. Simplified Sketch With Lever Added

$$y_b = r \left(\frac{r_s}{r_r} \right) \theta$$

so

$$y_b = r \left(\frac{r_s}{r_r} \right) \theta = r \left(\frac{r_s}{r_r} \right) \omega$$

and

$$y_b = r \left(\frac{r_s}{r_r} \right) \theta,$$

or

$$\theta = \left(\frac{r_r}{r_s} \right) \frac{y_b}{r}.$$

Let F = force between the spring and the lever

and F_r = force between the rotor and the lever.

Then, using a force balance on the lever:

$$F r_s = F_r r_r$$

or

$$F_r = F \left(\frac{r_s}{r_r} \right).$$

We will again write the three force equations and the initial condition for the linear and rotary impacts so we can easily compare them:

Impacting ball:

$$F = -M \ddot{y}_b$$

$$F = K (y_b - y_p)$$

$$F = (1/\alpha) \dot{y}_p$$

$$\dot{y}_{b0} = v_0$$

Impacting rotor with lever:

$$F_r r = -J \ddot{\theta} = F (r_s/r_r) r$$

$$F = - (J \ddot{\theta}/r) (r_r/r_s) = - (J r r_r \ddot{\theta}/r^2 r_s) = - (J r r_r /r^2 r_s) (r_r/r_s) (\ddot{y}_b/r) \\ = - (J/r^2) (r_r/r_s)^2 \ddot{y}_b$$

$$F = K [(r (r_s/r_r) \theta - y_p)] = K (y_b - y_p)$$

$$F = (1/\alpha) \dot{y}_p$$

$$r (r_s/r_r) \dot{\theta}_0 = r (r_s/r_r) \omega_0 = \dot{y}_{b0}$$

We see that we can make the two sets of equations identical by setting:

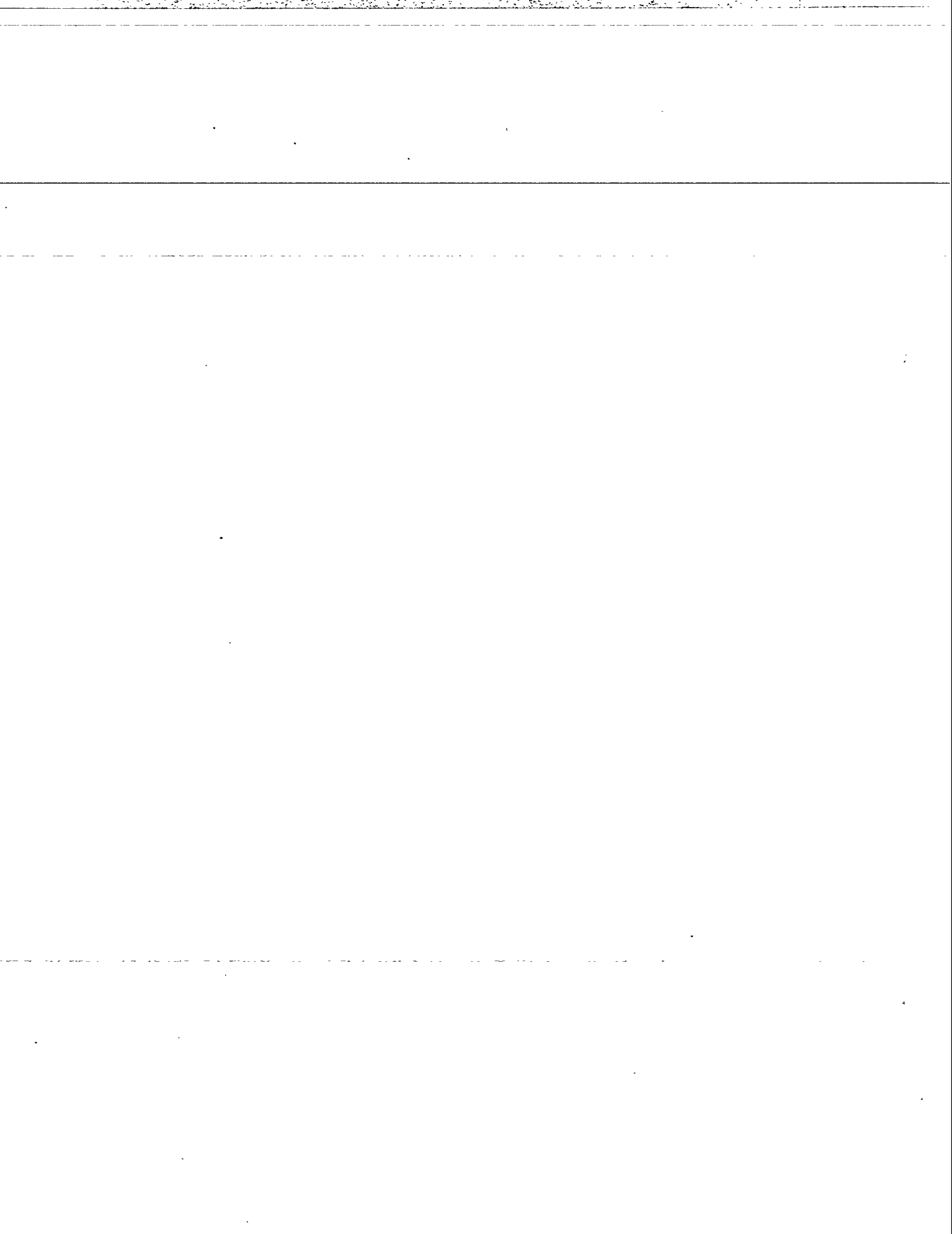
$$\frac{J}{r^2} \left(\frac{r_r}{r_s} \right)^2 = M$$

and

$$r \left(\frac{r_s}{r_r} \right) \omega_0 = v_0.$$

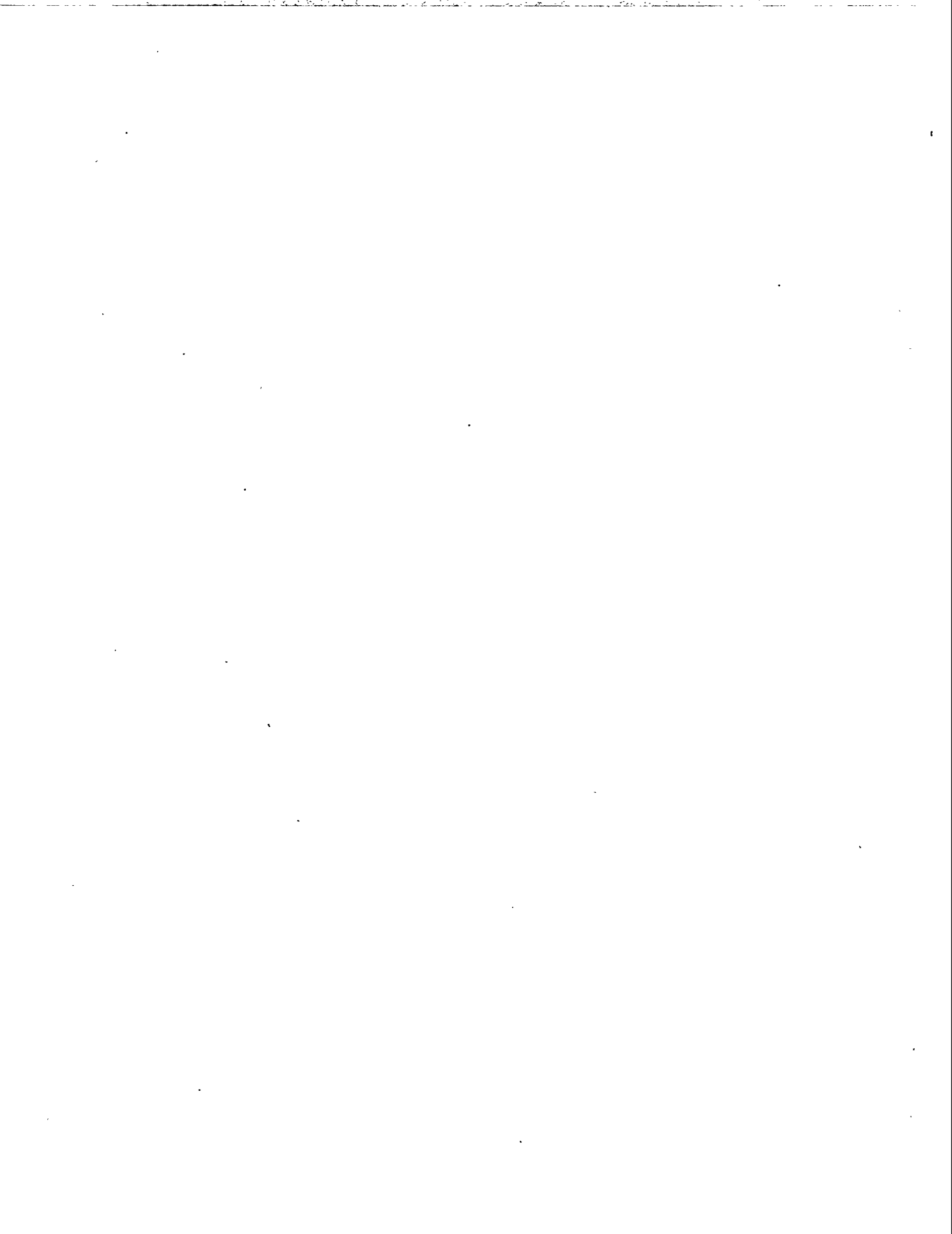
The lever can therefore further reduce the effective mass of the impacting object, thus further reducing the required plate size. Of course, we are also further increasing the effective velocity of the impact.

The box-shaped spring shown in Figure 2 is not a particularly simple device to design and build. We can delete that spring by simply making the lever arm nearest to the flat plate sufficiently flexible. We have analyzed the resulting mechanism to be sure of that conclusion, but we can get there much quicker with a few simple arguments. Since we have ignored the mass of the spring in our theory, it makes no difference whether the spring is considered to be attached to the flat plate or to the lever, as long as it acts between the end of the lever and the flat plate. The rigid lever arm with a spring attached to the end is mechanically equivalent to the flexible lever arm for small deflections. Although it is not so obvious, the box-shaped spring could also be deleted by making the other lever arm flexible, or making both arms flexible. The math would just get a little more complicated, and the results would be a little more difficult to interpret.



Appendix D

Dimensions and Units



Whenever masses and forces occur in the same engineering problem, the dimensions and units seem to get complicated. For this analysis, we have elected to eliminate the units of mass, expressing any masses in terms of force and acceleration.

We have used $(32.174 \text{ lbf} \cdot \text{ft} / \text{lbf} \cdot \text{sec}^2)(12 \text{ in.} / \text{ft}) = 386.09 \text{ lbf} \cdot \text{in.} / \text{lbf} \cdot \text{sec}^2$ for the conversion factor, so mass has the units of $\text{lbf} \cdot \text{sec}^2 / \text{in.}$ All dimensions are in terms of pounds-force (lbf), inches (in.), and seconds (sec), except for frequencies. For each parameter, the dimension is shown enclosed in square brackets. For dimensionless quantities, the dimension is shown as unity [1].

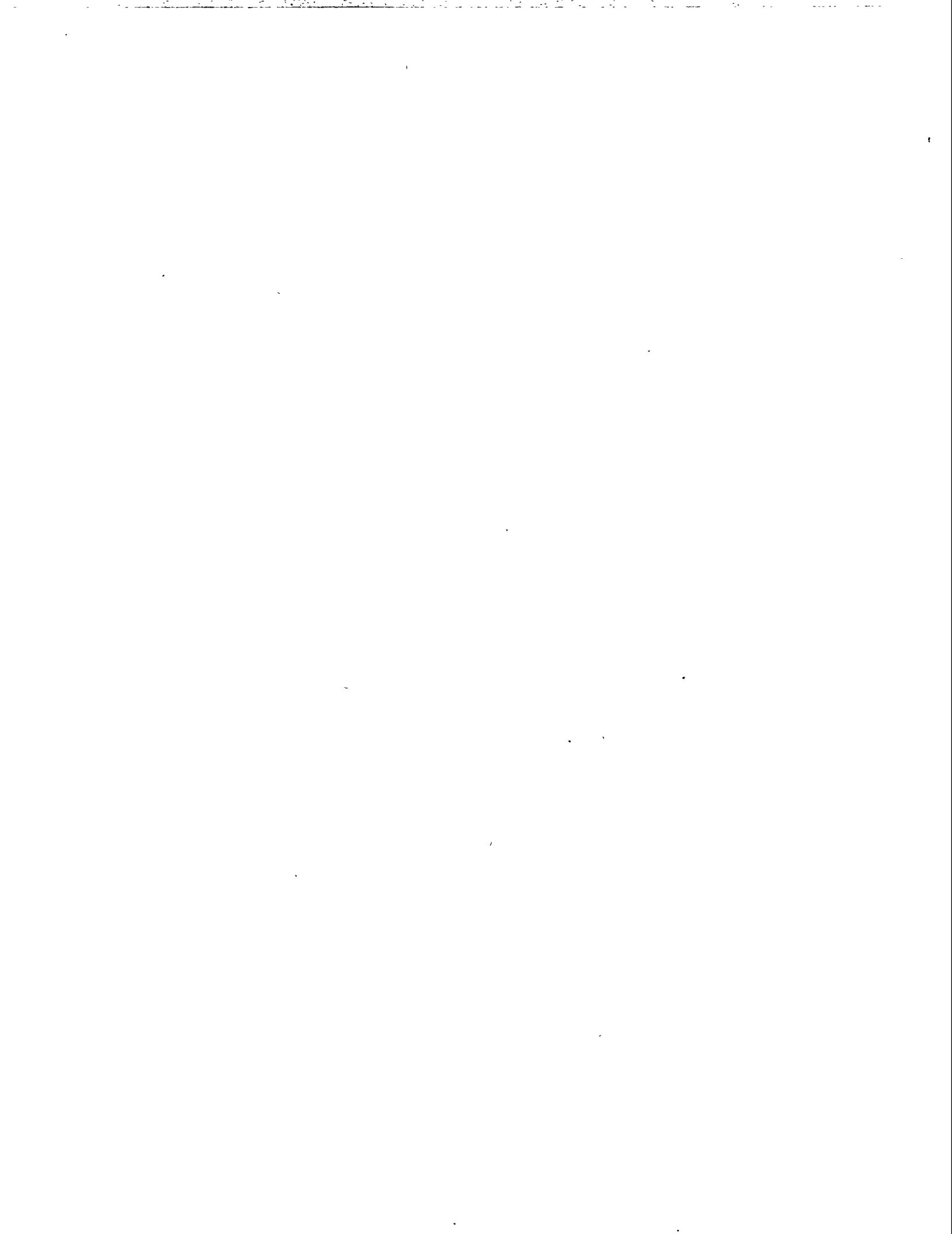
- C_g = group velocity of a flexural wave, the velocity at which energy is propagated [in./sec]
- C_{gi} = group velocity of an individual layer of a laminated plate [in./sec]
- C_p = phase velocity of a repeating flexural wave, the velocity of an infinite train of sine waves [in./sec]
- C_1 = first multiplier constant in the general solution for the deflection of the spring, x [in.]
- C_2 = second multiplier constant in the general solution for the deflection of the spring, x [in.]
- d_b = diameter of the ball dropped in the test [in.]
- D = plate modulus, a measure of the stiffness of the plate [lbf in.]
- D_i = plate modulus of an individual layer of a laminated plate [lbf in.]
- e = base of natural logarithms, approximately 2.7183 [1]
- E = modulus of elasticity of the plate material [lbf/in.²]
- E' = modified modulus of elasticity of the plate material, used when lateral dimensional changes are restrained, as in a plate [lbf/in.²]
- f = frequency of a repeating flexural wave [Hz]
- F = force applied between various elements of the flat plate device [lbf]
- F_r = force between the rotor and the lever in Appendix C [lbf]
- F_x = maximum value of force [lbf]
- g = local acceleration of gravity at the Kansas City Division [in./sec²]

- h** = thickness of the plate, if the plate has a single layer [in.]
 = thickness of an individual layer of the plate, if the plate has more than one layer [in.]
- h_b** = height of the bounce of the ball [in.]
- h_d** = height of the drop of the ball [in.]
- h_r** = relative bounce height, the ratio of the height of the bounce to the height of the drop [1]
- h_{rm}** = measured relative bounce height [1]
- H** = constant used in replacing C₁ and C₂ [in.]
- I** = another constant used in replacing C₁ and C₂ [in.]
- j** = $\sqrt{-1}$, used in expressing complex numbers [1]
- J** = mass moment of inertia of the rotating body in Appendix C [lbf in sec²]
- K** = spring rate of the linear spring element [lbf/in.]
- K_{fix}** = spring rate of the fixture when measuring K [lbf/in.]
- K_{meas}** = gross spring rate measured, before accounting for the spring rate of the fixture [lbf/in.]
- L_f** = distance traveled by the energy wave during the impact process [in.]
- l_s** = length of the side of a square flat plate [in.]
- m** = mass per unit plan-view area of the plate [lbf sec²/in.³]
- m_i** = mass per unit plan-view area of an individual layer of a laminated plate [lbf sec²/in.³]
- M** = mass of the ball which impacts the flat plate assembly [lbf sec²/in.]
- M_p** = mass of the flat plate [lbf sec²/in.]
- N** = number of identical layers of a laminated plate [1]
- q** = variable used in solving the differential equation of impact [sec⁻¹]
- r** = moment arm of the rotating body in Appendix C [in.]

- r_r = moment arm of the lever in Appendix C which is nearest the rotating body [in.]
 r_s = moment arm of the lever in Appendix C which is nearest the spring [in.]
 s = variable used in solving the differential equation of the impact [sec⁻¹]
 s_1 = value of s using the positive radical term [sec⁻¹]
 s_2 = value of s using the negative radical term [sec⁻¹]
 $s_{1,2}$ = values of s using \pm the radical term [sec⁻¹]
 S = plan-view area of the flat plate [in.²]
 t = time, measured from the beginning of the impact process, when the ball first makes contact with the spring [sec]
 t_b = bounce time in the tests, the time between the first and second impacts of the ball with the spring, used to determine the bounce height [sec]
 t_d = decay time of the plate [sec]
 t_f = time to the end of the impact process, when the spring is just no longer compressed [sec]
 t_u = time, in the impact process, until the flat plate has absorbed some fraction, ψ , of the initial kinetic energy of the ball [sec]
 t_x = time, in the impact process, until the spring deflection is a maximum [sec]
 T = the period of a repeating flexural wave [sec]
 U_{bu} = kinetic energy of the ball at time, t_u [lbf in.]
 U_{b0} = initial kinetic energy of the ball [lbf in.]
 U_{su} = potential energy of the spring at time, t_u [lbf in.]
 v_f = final velocity of the ball [in./sec]
 v_0 = initial velocity of the ball [in./sec]
 V_p = volume of the flat plate [in.³]
 x = deflection of the spring [in.]

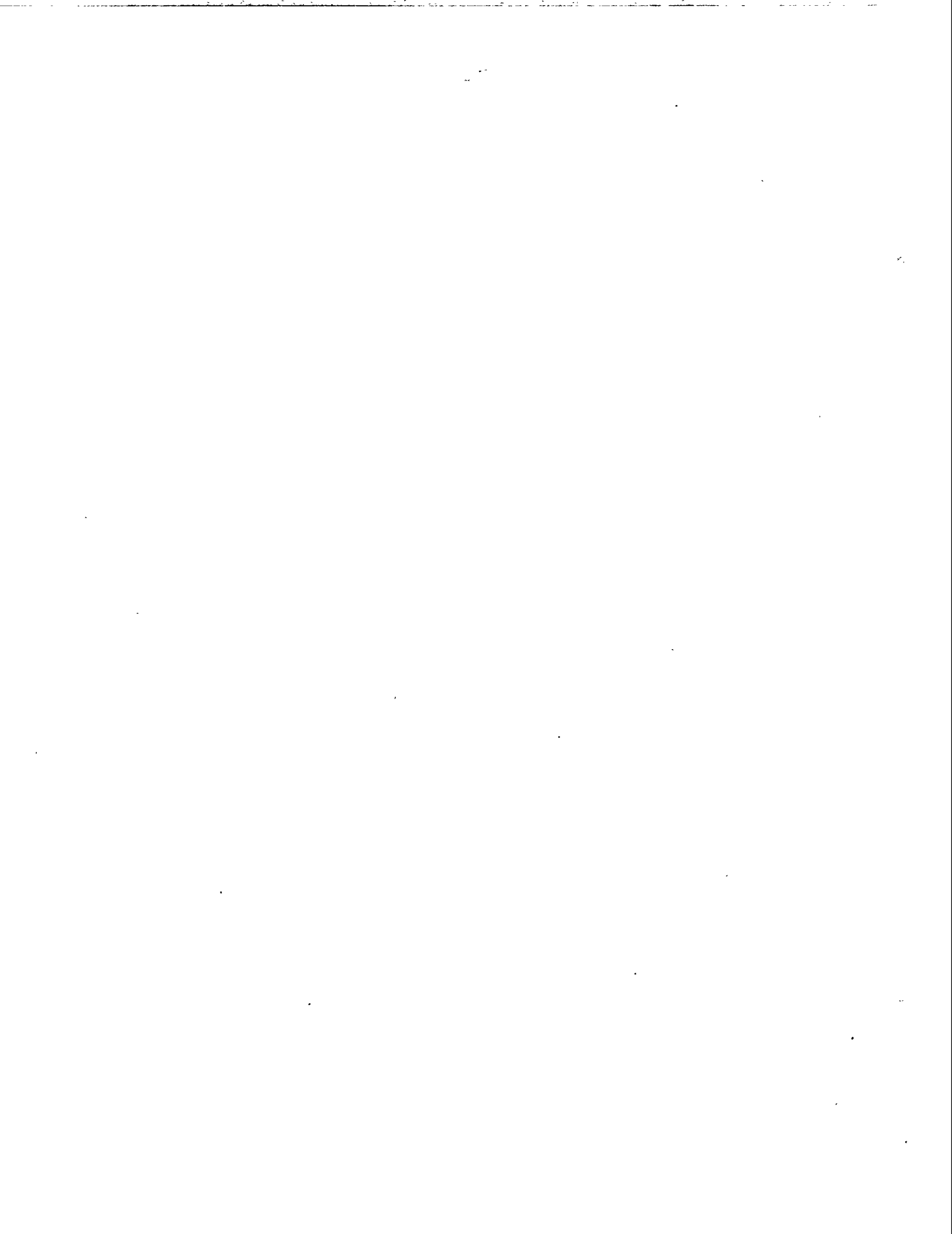
- x_f = deflection of the spring at the end of the impact process, defined to be equal to zero [in.]
- x_u = deflection of the spring at time, t_u [in.]
- x_x = maximum deflection of the spring [in.]
- x_0 = initial deflection of the spring, defined to be equal to zero [in.]
- \dot{x} = first derivative of the spring deflection, x , with respect to time [in./sec]
- \dot{x}_f = value of \dot{x} at the end of the impact process [in./sec]
- \dot{x}_x = value of \dot{x} when the spring has the maximum deflection [in./sec]
- \dot{x}_0 = value of \dot{x} at the beginning of the impact process [in./sec]
- \ddot{x} = second derivative of the spring deflection, x , with respect to time [in./sec²]
- y_b = displacement of the ball (or other impactor) from its position at initial contact with the spring [in.]
- \dot{y}_b = first derivative of y_b with respect to time [in./sec]
- \dot{y}_{bu} = first derivative of y_b with respect to time at time, t_u [in./sec]
- \dot{y}_{b0} = value of \dot{y}_b at the beginning of the impact process [in./sec]
- \ddot{y}_b = second derivative of y_b with respect to time [in./sec²]
- y_p = displacement of the center of the flat plate from its position at the beginning of the impact process [in.]
- y_{px} = maximum value of y_p [in.]
- \dot{y}_p = first derivative of y_p with respect to time [in./sec]
- \ddot{y}_p = second derivative of y_p with respect to time [in./sec²]
- α = property of a thin flat plate, shown by Zener to act as the inverse of a viscous damping coefficient [in./lbf sec]
- α_i = α for an individual layer of a laminated plate [in./lbf sec]
- β = variable used in calculating the value of t_u for a given test condition for a square flat plate [sec^{0.5}]

- γ = another variable used in calculating the value of t_u for a given test condition [sec^{0.5}]
- η = relative bounce height when energy reflected from the edges of the plate is not considered [1]
- θ = dimensionless real variable used in Euler's equation [1]
- θ = angle of rotation of an object in Appendix C, from its position at the beginning of the impact process [radians = 1]
- θ_u = $q t_u$ [1]
- $\dot{\theta}$ = first derivative of the angle of rotation, θ , of an object in Appendix C with respect to time [radians/sec = sec⁻¹]
- $\dot{\theta}_0$ = value of $\dot{\theta}$ at the beginning of the impact process [radians/sec = sec⁻¹]
- $\ddot{\theta}$ = second derivative of the angle of rotation, θ , of an object in Appendix C with respect to time [radians/sec² = sec⁻²]
- λ = dimensionless grouping of the elements of the impact problem [1]
- Λ = wavelength of a repeating flexural wave [in.]
- μ = $\sqrt{4 - \lambda^2}$ [1]
- ν = Poisson's ratio of the plate material [1]
- π = 3.14159..... [1]
- ρ = density of the plate material [lbf sec²/in.⁴]
- σ_x = maximum mechanical stress in the flat plate, in Appendix F [lbf/in.²]
- ψ = relative bounce height when only the energy reflected from the edges of the plate is considered [1]
- ω = circular frequency of a repeating flexural wave [radians/sec = sec⁻¹]
- ω = $\dot{\theta}$ = first derivative of the angle of rotation, θ , of an object in Appendix C with respect to time [radians/sec = sec⁻¹]
- ω_0 = $\dot{\theta}_0$ = first derivative of the angle of rotation, θ , of an object with respect to time at the beginning of the impact process, in Appendix C [radians/sec = sec⁻¹]



Appendix E

Flat Plates Which Cause Cancellation of First Reflections From the Edges



It seems that any regular polygon with an even number of sides would cause cancellation of first reflections from the edges, as long as half of the edges were supported and half were free and the impact occurred at the center of the plate. Each edge would then subtend an equal angle of the flexural energy wave, and the reflection from each supported edge would be equal and opposite to that from each free edge. Thus, with a square plate, two adjacent sides could be supported or two opposite sides, but having the supports on opposite sides seems to be mechanically better. There also doesn't seem to be a good mechanical reason to go to more than four sides.

An arrangement which may have some advantages is shown in Figure 1. Basically, two square flat plates are joined together along a common side, and equal and opposite impacts are delivered to the centers of the two plates. The flexural energy waves are not reflected from the common edge, but each continues on into the other plate. The waves are, however, equal and opposite so the net effect is identical (it seems) to having each wave reflected from the common edge as if it were a supported edge. We can think of the common edge as having a virtual support and can consider each square half of the plate as if the other half weren't there, each half of the plate impacted with half of the total mass. We showed earlier that the required plan-view area for a flat plate is directly proportional to the mass of the impacting object. Therefore, each half-mass would require a half-area and the total area of the plate would be the same as if only a single square plate were used.

The rectangular shape itself may be advantageous in some applications, but the concept also allows a fairly simple way to apply the flat plate device to a miniature mechanism. Figure 2 shows a sketch of a flat plate device which will be impacted by an arm of a rotating device. The impact is simply shown as an arrow in the interests of clarity. The structure between the impact and the flat plate serves as a pair of levers and a pair of springs, delivering equal and opposite impacts to the two halves of the flat plate. The levers reduce the effective mass of the impact, allowing a smaller flat plate; and the spring rates of the arms are chosen to minimize the bounce.

The structure will pivot about the axis indicated, for the following reasons: The pivot point must be located on the mid-plane of the flat plate because of the lateral rigidity of the flat plate. Since each arm is connected to the center of each half-plate and each arm has the same spring rate, the pivot point must also be located midway between the connections to the flat plate, because of symmetry. The impact doesn't have to occur directly above the pivot point.

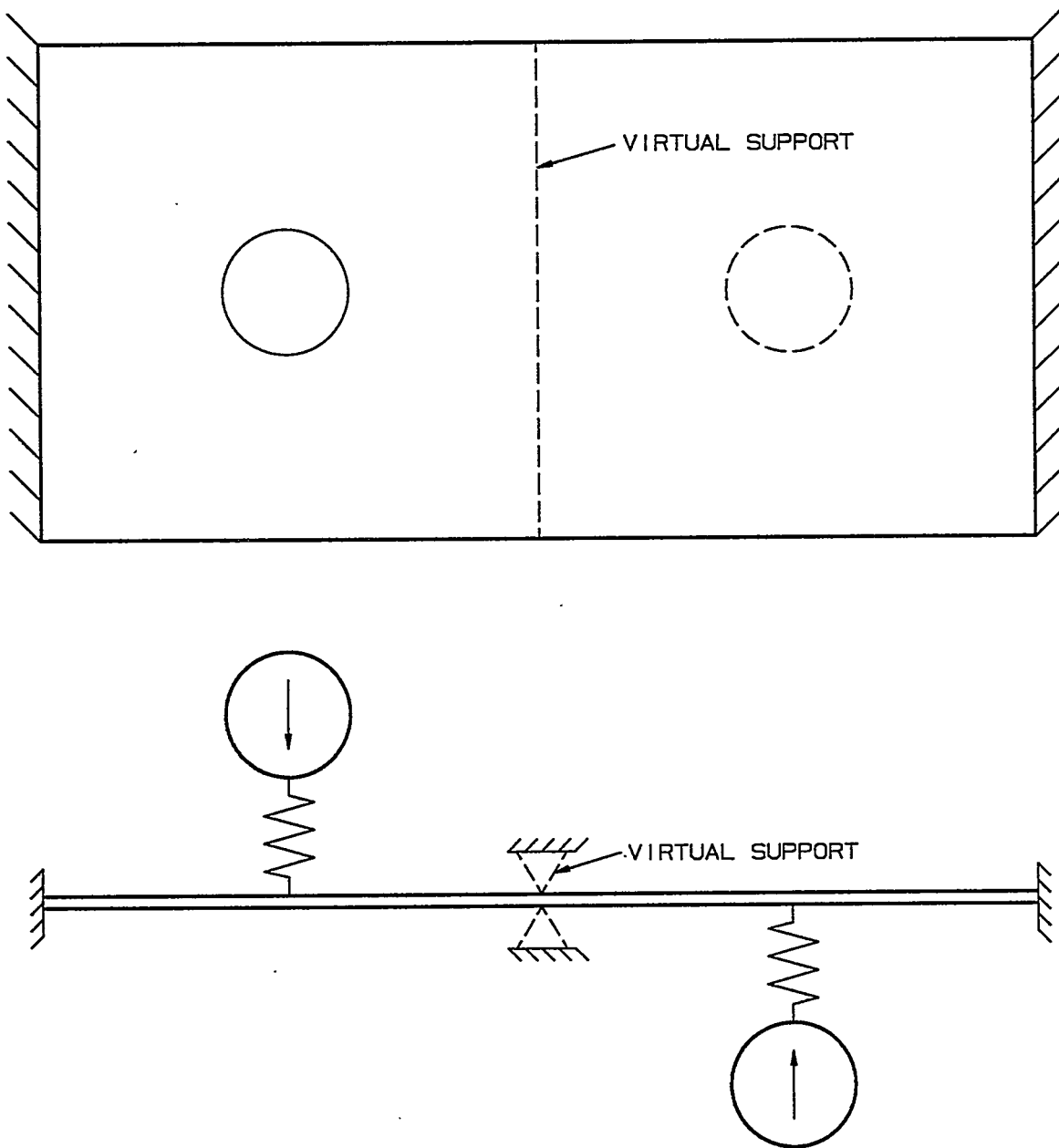


Figure 1. Rectangular Plate With Virtual Support

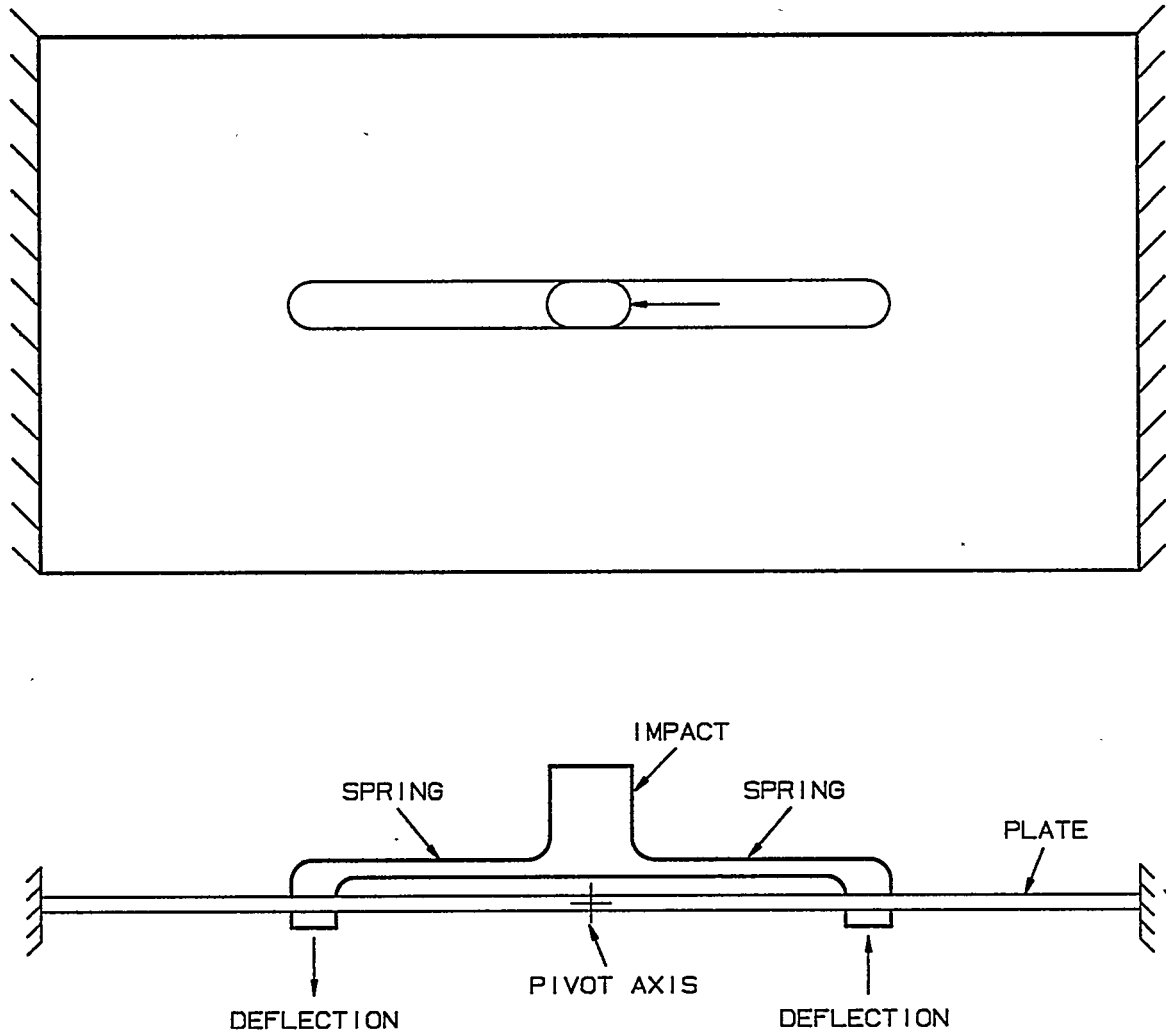
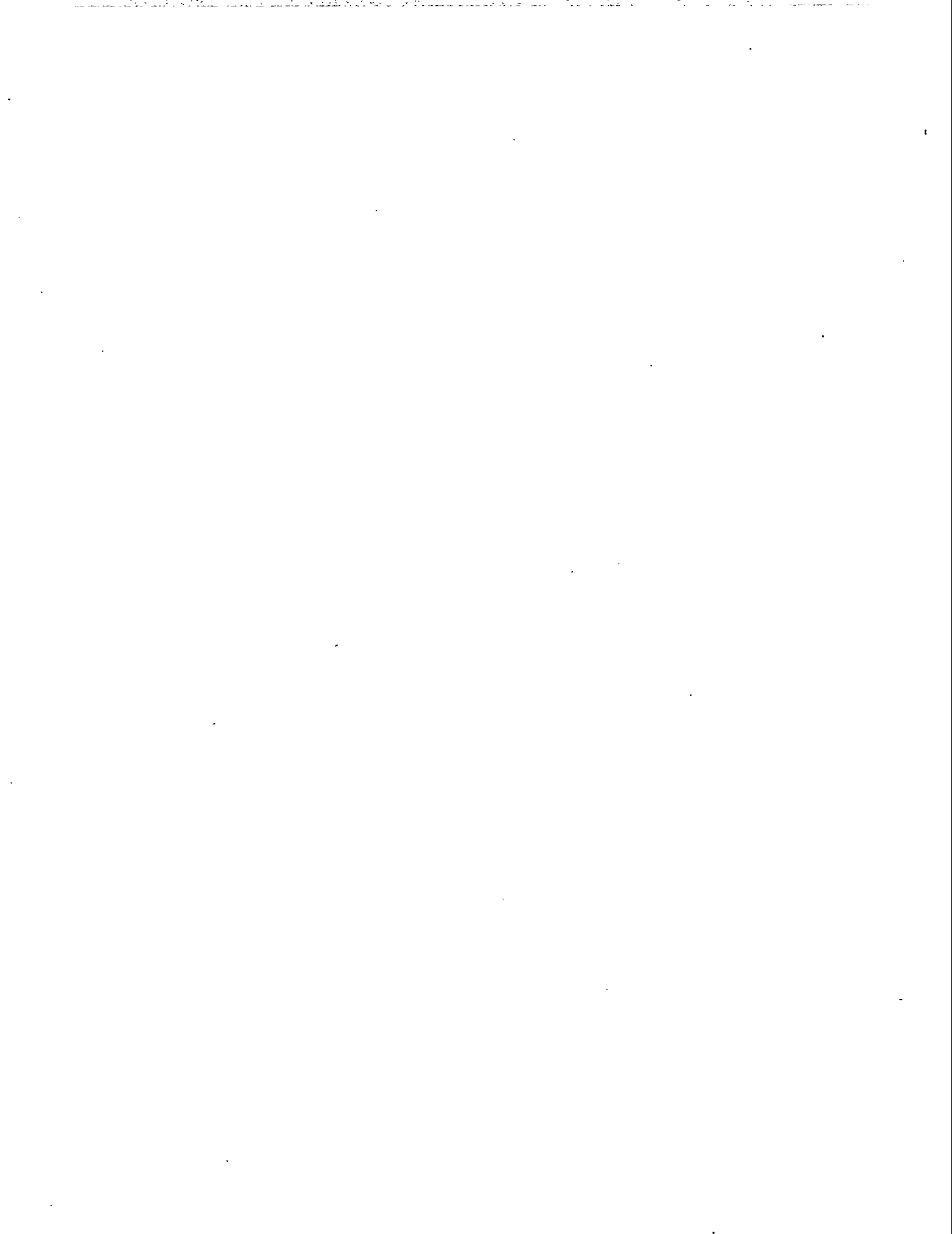
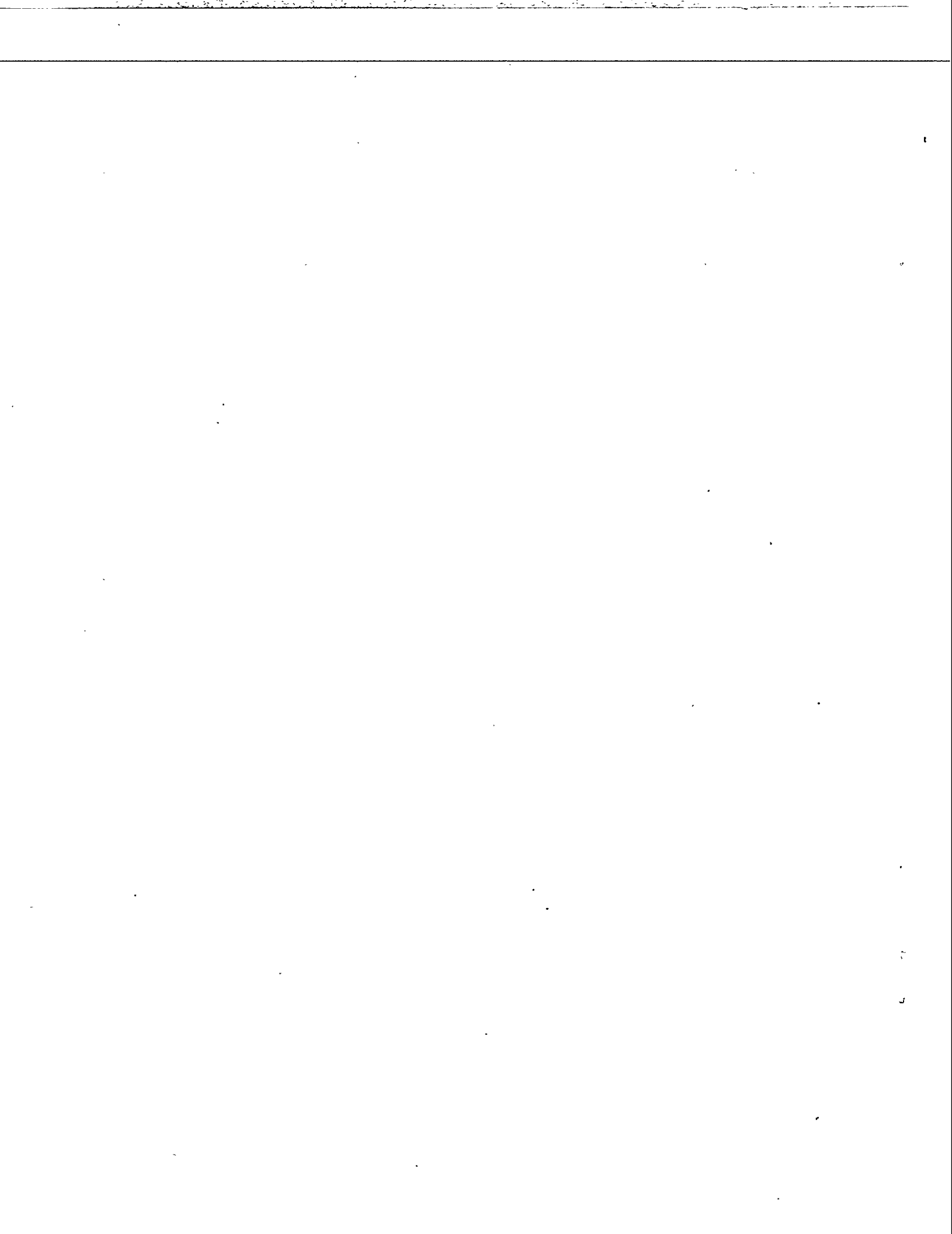


Figure 2. Flat Plate Device for Miniature Mechanism



Appendix F
Scaling the Flat Plate Device



When we chose to test flat plate devices by dropping balls onto them, we decided it would be too difficult to test the small flat plates which would be applicable to the miniature mechanisms we were interested in. We therefore applied modeling principles to allow us to use plates which were about three times larger in all dimensions. Of course, we also used balls which were scaled up. In order to justify the modeling, we will walk through the procedure and use the results in the application of our test data to a reduced-size flat plate.

We will basically follow the discussion of dimensional analysis and modeling in Eshbach's handbook.⁶ We should first list all of the quantities which relate to the problem, but we can significantly reduce the size of that list by deleting those which are defined in terms of others. Since we are going to find that all quantities which have the same dimension will scale the same, we can just select a representative length, velocity, force, etc. Also, any dimensionless numbers, such as N and ν , will have scale factors of one, so we won't list them.

Any problem in mechanics requires three fundamental units (which we have chosen to be inches, seconds, and pounds-force), and this entitles us to arbitrarily scale any three of our quantities, as long as they are dimensionally independent. We will select h as one of the three because we want to scale the linear dimensions of the problem, say to half size. We will also select E and ρ because they are the only material properties of the flat plate which have dimensions. This allows us to keep the same materials for the reduced-size flat plate as were used in our tests, by making their scaling factors unity.

The remaining quantities were chosen to be F_x , K , M , S , t_f , U_{b0} , v_0 , V_p , \ddot{y}_b , σ_x , and ω ; a total of eleven. (The quantity, σ_x , may look unfamiliar, since we haven't used it anywhere in this report. We will take it to be the maximum mechanical stress in the flat plate, at some unknown location and time.) We therefore have to form eleven independent dimensionless groups of quantities. An easy way to ensure independence is to use a single one of the eleven quantities in a given dimensionless group, along with one or more of the quantities h , E , and ρ . We could set up equations involving exponents of units to find these groups, but we can do it more easily by inspection. We find the following dimensionless groups:

$$\frac{F_x}{E h^2}; \frac{K}{E h}; \frac{M}{\rho h^3}; \frac{S}{h^2}; \frac{t_f}{h} \sqrt{\frac{E}{\rho}}; \frac{U_{b0}}{E h^3}; v_0 \sqrt{\frac{\rho}{E}}; \frac{V_p}{h^3}; \frac{\rho h \ddot{y}_b}{E}; \frac{\sigma_x}{E};$$

and

$$\omega h \sqrt{\frac{\rho}{E}}.$$

The next step is to replace each quantity in each of the above groups with the scaling factor for that quantity, then set that new group equal to one. We will enclose each quantity in parentheses to indicate the scale factor for that quantity.

So far, we have set $(h) = 0.5$, $(E) = 1$, and $(\rho) = 1$.

Then,

$$\frac{(F_x)}{(E)(h^2)} = 1,$$

or

$$(F_x) = (E)(h^2) = (1)(0.5^2) = 0.25.$$

We can skip a step for the rest and find:

$$(K) = (E)(h) = (1)(0.5) = 0.5,$$

$$(M) = (\rho)(h^3) = (1)(0.5^3) = 0.125,$$

$$(S) = (h^2) = (0.5^2) = 0.25,$$

$$(t_f) = (h) \sqrt{\frac{(\rho)}{(E)}} = (0.5) \sqrt{\frac{1}{1}} = 0.5,$$

$$(U_{b0}) = (E)(h^3) = (1)(0.5^3) = 0.125,$$

$$(v_0) = \sqrt{\frac{(E)}{(\rho)}} = \sqrt{\frac{1}{1}} = 1,$$

$$(V_p) = (h^3) = (0.5^3) = 0.125,$$

$$(\ddot{y}_b) = \frac{(E)}{(\rho)(h)} = \frac{1}{(1)(0.5)} = 2,$$

$$(\sigma_x) = (E) = 1,$$

and

$$(\omega) = \frac{1}{(h)} \sqrt{\frac{(E)}{(\rho)}} = \frac{1}{0.5} \sqrt{\frac{1}{1}} = 2.$$

It is obvious from the above procedure that any length would have a scale factor of 0.5, any velocity a scale factor of 1, etc., and that any dimensionless number would have a scale factor of 1.

These scale factor results are used in two different ways, depending on the quantity. Some tell us how we must control the half-size tests and some predict results of the half-size tests. For example, the v_0 scale factor of 1 tells us that we must use the same initial velocity for the ball in the half-size tests as we used in the full-size tests in order to be sure the results will scale properly. The σ_x scale factor of 1 tells us that the maximum mechanical stress in the half-size flat plate will be the same as that in the full-size flat plate, even though we have no idea of what it might be.

There are some other interesting results. The decay time of the flat plate will only be half as long, so we may have to use different recording equipment, or at least run the Visicorder faster. The group velocity of the flexural wave will scale the same as the initial velocity of the ball, even though they are entirely different kinds of physical processes.

One result warns us that we really can't scale the entire test setup! Since \ddot{y}_b has a scale factor of 2, the local acceleration of gravity, g , must be twice as great for the half-size tests as it was for the full-size tests. However, it doesn't take us long to realize that we are really only interested in the initial velocity of the ball, not the height it was dropped from. We can then exclude the local acceleration of gravity from the problem we are modeling and calculate the proper drop height for the half-size tests without referring to modeling theory. The ratio of bounce height to drop height is dimensionless, so it will be the same in the half-size tests as it was in the full-size tests.